ABSTRACT

The vast majority of passenger vehicles in the world are powered by fuel extracted from crude oil reserves. By 2050, the number of such vehicles would reach around 2.5 billion. As the conventional crude oil reserves are getting scarce by the very day, the demand for alternative fuels is thriving. Alongside which the engine modification has reached a limiting value thus giving a meagre scope for further research. Also, many countries across the globe have implemented policies to promote zero-emission vehicles adoption. These issues have paved the way for new technologies like fuel cell, battery electric vehicle, and supercapacitor. Battery technology is at its peak research since it is a quintessential and a flexible power source for almost all electrical and electronic technology. Future of Battery Technology is at the heart of the battery electric vehicle's research and development. But despite its merits, it faces a lot of setbacks such as thermal management and cooling, energy density (energy to size or mass), fast charging and proper storage. This project performs an analysis of heat generation in single cell Lithium-ion batteries and its cooling using various cooling liquids viz. Air, Water, Water- Ethylene Glycol (7%) and Water-Al_2O_3 through a special arrangement using SimScale software. Mathematical modeling for temperature distribution and conjugate heat transfer from cell core to cooling fluid is studied.

CONTENTS

List of Figures

List of Tables

Chapter 1

Introduction

CHAPTER 1
INTRODUCTION

Under the pressure of greenhouse gas and energy shortage, the electrification of transport plays an important role to meet the objective of the Paris Agreement enforced in November 2016. One of the technologies chosen to meet this objective is Lithium-ion Batteries (LIB). Lithium-ion batteries are being used in almost all fields of electric and electronic systems because of their superior properties. Electric vehicles, consumer electronics, aerospace industries are the fields where they are used heavily. High capacity, high efficiency, long life, low self-discharge, high energy density [1,2] makes them distinct from others. But despite this advantage, they pose some serious problems like thermal management and cooling, size and compatibility, high charging time. Generally, a large number of batteries are densely arranged into a battery pack to meet the requirement of higher power density which would lead to severe thermal management issues on account of the heat accumulation inside the battery pack.

The safe and efficient range of working temperature for lithium-ion batteries is around 0°C to 40°C, but it can go as high as 60°C. Above this range, there will be a phenomenon of thermal runaway where an increase in cell temperature leads to further increase in temperature thus ending in failure of the cell. The thermal runaway follows a mechanism of chain reactions, during which the decomposition reaction of the battery component materials occurs one after another.

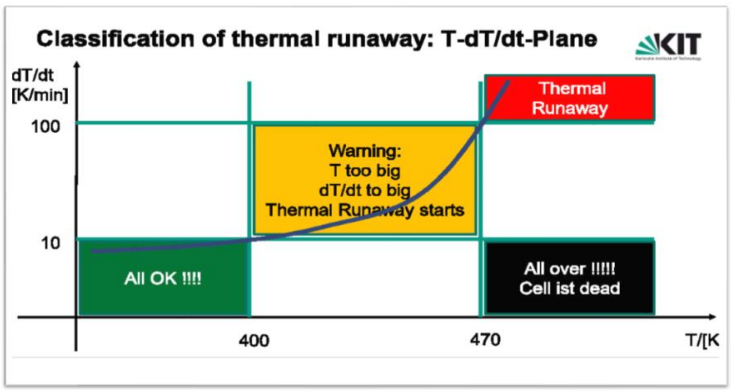

Figure 1.1 : Classification of Thermal Runaway

Also, while designing a module structure and choosing a cooling method, trade-offs need to be made among various factors such as cost, complexity, weight, cooling effects, temperature uniformity, and parasitic power. A driving factor for Li-ion battery modelling is the demand from system-level design and simulation in electric vehicle applications. Recently, several battery models are being introduced and studied in automobile applications. They can be classified as electrochemical, mathematical, electrical, and polynomial. All these models have the ability to predict the performance of the battery, but with different levels of simplicity and accuracy. Thus, a keenly designed module structure and cooling method should maintain the temperature within the operating range.

Chapter 2
Literature Survey

CHAPTER 2
LITERATURE SURVEY

Being a topic of interest among applied scientists and of great relevance in industry; a lot of information is available in literature. Tao Wang et.al [1] have worked regarding cooling of cell packs using forced air convection. They tested forced air convection in 5×5 rectangular array of cells, 19 cells hexagonal arrangement and 28 cells circular arrangement. Lumped model is used for analysis. They used CFD techniques to get the results and simulated using Ansys Icepack™ which was verified using experimental technique. By varying cell distance and orientation, they obtained different set of results. The peak temperature rose up to 36°C. Jingzhi Xu et.al [2] studied thermal management of fat plate and cylindrical lithium-ion cells using a specially designed arrangement of cells. By varying channel size and number of channels effect on cooling is studied. As the number of channels is increased there is unevenness in temperature distributions. By varying Reynold's number and charge-discharge rate heat generation and its dissipation is studied.

Naixing Yang et.al [3] developed a thermal model of lithium-ion cell using appropriate electrochemistry theory. Using governing equations and solving them they found cell temperature profile and heat transfer. They studied effect of staggered arrangement and longitudinal interval arrays. Ali.M.Sefidan et.al [4] formed a pseudo-2-D simulated model of lithium 18650 lithium ion battery. Initially, they analysed heat generated for different discharge rate and maximum temperature rise as per thermal-electrochemistry model. They placed lithium ion cell in a cylindrical tank comprising of Al_2O_3 Nano particles embedded in water as base fluid. These secondary cylinders were arranged in certain manner and cooled using forced air convection. Study is conducted in critical arrangements which are much vulnerable to thermal runway and potentially dangerous. By varying arrangements, Reynold's number the effects are studied. A peak temperature of 57°C is seen at critical areas without cooling and a maximum temperature 32°C is seen with implementation of cooling method.

Yang Li et.al [5] set up an experimental method to determine heat transfer and most efficient way of thermal management using indirect cooling and nanofluids like TiO, ZnO and diamond particle nanofluids with 50% distilled water and 50% ethylene glycol as base fluids. They placed 7 tractive lithium ion batteries and U-shaped copper tubes were attached to the walls of cell in which nanofluids where made to flow to enhance heat transfer. Among the three nanofluids diamond based nanofluid gave excellent result like stability over working temperature quick heat absorption and dissipation. These arrangements made discharge cycle much stable and heating of cell was effectively reduced. Long Cai et.al [6] simulated electrochemistry and thermal modelling of lithium 18650 cells using COMSOL Multiphysics 5.3a™. They considered more than 30 factors including chemical and thermal properties. This helps to understand heat generation and behaviour of cell under charge and discharge cycle.

C.Ziebert-A.Melscher et.al [7] studied different heat generation model experimentally. Adiabatic model, isoperibolic model, reversible and irreversible heating model are the three modes of heat generation models. They developed mathematical modelling for the above and found maximum heating range and temperature using Battery Calorimeter. They also simulated these results using COMSOL Multiphysics 5.3a™ in order to study thermal runaway in cells.Leyuan Yu et.al [8] conducted heat transfer studies in Alumina-Polyalphaolefin based nanofluids having spherical and non-spherical (nano-rods). The nanofluid is synthesized with 3% of volume fraction for spherical nanofluid and 1% volume fraction for nano-rods. Effective viscosity and effective thermal conductivity were measured and compared with standard results. It was determined that aspect ratio, shear field, aggregate dispersion, volume fraction, are key factors that determine nanofluid properties. Certain correlations were used from literature in determining various parameters. Pressure drop and overall heat transfer coefficient were the output result and results were validated experimentally and compared with previous studies. Results were satisfactory for spherical nanofluids but were not for non-spherical.

S.Suresh et.al [9] synthesized $Al_2O_3 - Cu$ water hybrid nanofluid and studied their properties in laminar convective heat transfer. Using Hydrogen reduction technique nanofluids were synthesized with 0.1% volume fraction of nanoparticles in deionized water as base fluid. These fluids were made to flow in circular heated tube. Pressure drop and heat transfer coefficient were noted and Nusselt's number was determined. There was an increase of 13.56% of Nusselt's number at a Reynold's number of 1730 when compared to that of ordinary water. There was an increase of about 10.94% heat transfer overall which indicates superior quality of hybrid nanofluid.

Bittogopal Mondal et.al [10] studied effect of nanofluids in cooling of lithium-ion batteries using two different flow configurations. Temperature distribution heat dissipation, flow characteristics were extensively studied using experimental and analytical methods. Nanofluids like ethylene glycol-water, alumina-water, ethylene glycol-CuO hybrid fluids where used in study.

Adnan.M.Hussain et.al [11] conducted experiments on effect of nanofluid in automobile cooling. They used $SiO_2\ and\ TiO_2$ water based nanofluids in car radiator. They performed experiment by varying discharge rate from 2-8LPM, inelt temperature 60-80°C and nanofluid concentration of 1-2% by volume. They found an increase in Nusselt's number with as discharge rate is increased thus, there was increased heat transfer. There was slight increase in Nusselt's number by increasing inlet temperature and volume concentration.

Chapter 3

Objective and Scope of Present Work

CHAPTER 3
OBJECTIVE AND SCOPE OF PRESENT WORK

3.1 OBJECTIVE

In the current project,

Thermal control of lithium-ion batteries is one of the most important aspects of their application. The temperature can vary due to internal factors and due to the external environment. If the cell temperature is not controlled the cell will go into a phenomenon of thermal runaway where cell temperature increase causes a further rise in temperature thus causing the overall failure of the cell. If this has to be prevented sufficient cooling thas to be provided. So in order to develop an efficient cooling method, it is necessary to the ideas and concepts behind it.

In order to study the cooling of lithium-ion cells; initially one has to study the thermal and chemical effects that are responsible. Lithium 18650 cell was considered for analysis. Lithium-ion cell works under redox reaction. So different mode of heat generation in lithium-ion cells due to various contributing factors are studied. Once the heat generation is known using governing equation temperature distribution across the cell is found. Once the temperature is known the heat transfer between cell and fluid can be found out. Certain assumptions are made in order to make the formulation of problem simple.

The mathematical model is used to understand the fundamentals and working principle of heat transfer from the cell surface to the fluid. Considering the entire cell surface at constant temperature heat transfer in a small duration is calculated. The models are developed for both static conditions i.e. free convection and dynamic condition i.e. forced convection of coolant fluid. Different dimensionless numbers like Nusselt's number, Prandtl's number Rayleigh number, Reynolds number are evaluated to determine various properties and conditions. By balancing heat transfer fluid temperature is found. Once we get fluid temperature, we find the new value of cell temperature for iteration

Opensource cloud-based software Simscale is used for simulation. 3-D cad modeled using CATIA V-5. The 3-D model was imported to Simscale. Conjugate heat transfer module was used since the heat transfer is between solid and liquid through their phase interface. The hex-dominant auto mesh is used to mesh the entire setup. An arrangement of 16 cells was made in a 4×4 matrix and coolant fluid is made to flow along the direction of the symmetry axis of the cell. The simulation was done for different cases by varying the discharge rate of cell and fluid velocity of the cells. The discharge rate of 1C, 2C, 3C discharges were considered, different types of coolant fluids were used and velocity of the fluid is varied from 0.01m/s, 0.05m/s, 0.5m/s, and 1m/s. Air, water,water-ethylene glycol(7%) and water-Al_2O_3based nanofluids were used as coolants. Temperature hot spot regions are analyzed and overall cooling is found. After simulation optimum velocity and suitable coolant is found for all discharges.

3.2 SCOPE OF PRESENT WORK

In an era of depleting oil reserves, the turmoil of the energy crisis is getting worse every year. The electric vehicles are gaining importance. These vehicles use mainly lithium ion 18650 cells. These cells have certain limitations. Thermal runaway is the main problem which leads to the failure of the cell. Temperature control plays an important role. Thus there is a need for proper cooling of the cells by the circulation of the coolants around the cells.

In this project we studied the mathematical model for heat transfer model. We implemented the project by considering four fluids namely, air, water, water – ethylene glycol (7%) and water – 1% Al_2O_3.

3.3 LAYOUT OF THESIS

This thesis is divided into eight chapters. The layout is outlined below:

- In chapter 1 the concept of thermal runaway in batteries is introduced.
- In chapter 2 background of battery cooling, the importance of external cooling, use of various fluids including nanofluids and temperature distribution in the fluid flow simulation is studied.

- In chapter 3, the objectives of current work and scope of present study and contribution of this thesis are indicated.
- In chapter 4, electrochemical model of cell along with cell reaction is studied and various heat generation models are explained. The mathematical model of temperature gradient of cell is derived. Conjugate heat transfer fundamentals are studied. The flowchart for mathematical model is given. Introduction to nanofluids and synthesis of nanofluids are explained.
- In chapter 5, a brief introduction of SimScale, its pre-processing, simulation and post processing are explained. Simulation methodology is explained in brief.
- In chapter 6, the results of simulation is discussed. Table for various coolants consisting of velocity, discharge rates and maximum temperature is also given.
- Finally, Chapter 7 summarizes the present work. Also the scope of future work is discussed.

Chapter 4

Theoretical Model

CHAPTER 4

THEORETICAL MODEL

4.1 ELECTROCHEMICAL MODEL

A lithium ion cell works under the principle of a redox reaction. It has Li and oxides of some metal as electrodes. During the charging cycle, Li-ions will move from the positive electrode and are deposited into the negative electrode. Reverse process will occur during the discharge cycle. The cell reaction is given as in Eq. (1) [7] for Li-ion cell with CoO_2

Anode: $Li \rightarrow Li^+ + e^-$

Cathode: $CoO_2 + Li^+ + e^- \rightarrow LiCoO_2$

Overall: $CoO_2 + LiC_6 \rightarrow LiCoO_2 + C_6$ ...(4.1)

Positive Electrode: $LiCoO_2$ on 10-25mm thick Al Foil

Negative Electrode: Graphite on 10-12mm thick Cu Foil

Separator: 16-25mm thick POLYOLEFINE MEMBRANE (PE, PP, PE/PP)

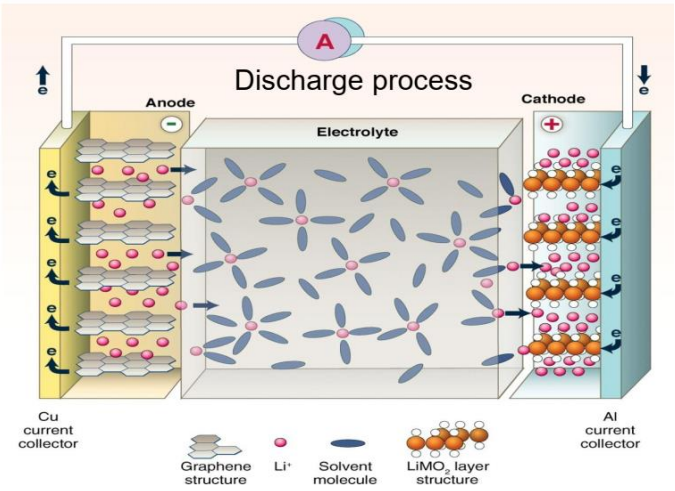

Figure 4.1 : Schematic diagram of Lithium-ion cell

4.2 VARIOUS HEAT GENERATION MODEL

4.2.1 Adiabatic Measurement

No heat exchange between cell and surrounding. Cell temperature increases rapidly until the cell breaks down due to thermal runaway.

$$\dot{Q}_{gen} = mc_p \frac{dT}{dt} \quad \textbf{...(4.2)}$$

4.2.2 Isoperibolic Measurements

Approximately isothermal conditions; the outer environment is maintained at a constant temperature. [6]

$$\dot{Q}_{gen} = mc_p \frac{dT}{dt} + Ah(T_s - T_c) \quad \textbf{...(4.3)}$$

4.2.3 Measurement of Reversible & Irreversible heat

This includes heat generated due to Joule heating effect which is irreversible and second term due to entropy changes which are reversible.

$$\dot{Q}_{gen} = -I(E_0 - E) - IT\frac{dE_0}{dT}$$

This can be also re- written as

$$\dot{Q}_{gen} = i^2R - T\Delta S\frac{i}{nF} \quad \textbf{...(4.4)}$$

$$Q_{gen} = Q_{Electrochemical} + Q_{Exothermic} \quad \textbf{...(4.5)}$$

4.3 MATHEMATICAL MODEL OF TEMPERATURE GRADIENT

Figure 4.2 : Plane View of cylindrical battery

For the purpose of analysis let us consider the cylindrical lithium-ion cell as a cylinder with heat generation at its centre. Certain assumptions are made to simplify the analysis:

- Only radial conduction is assumed.
- Heat conduction due to radiation is neglected. Complete heat gets transferred to coolant fluid in contact.
- Material is isotropic.
- Heat is generated at the center and distributed radially which is a function of time and position (radius).
- Variations of parameters like density, viscosity, etc. are neglected and their average values over working range are taken.

The general heat transfer equation is given as follows:

$$\nabla^2 T + \dot{Q}_{gen} = \frac{1}{\alpha}\frac{\partial T}{\partial t} \qquad \text{...(4.6)}$$

Considering only radial heat transfer to obtain temperature distribution across the cell

$$\frac{1}{r^2}\frac{\partial}{\partial r}\left(r\frac{\partial T}{\partial r}\right) + \dot{Q}_{gen} = \frac{1}{\alpha}\frac{\partial T}{\partial t} \quad \textbf{...(4.7)}$$

This is in the form of $\boldsymbol{T(r,t) = G(r).S(t)}$; which is a partial differential equation and homogenous and non-homogenous are solved separately.

4.3.1 Solving the non-homogenous part

$$\frac{1}{r^2}\frac{d}{dr}\left(r\frac{dT}{dr}\right) = -\frac{\dot{Q}_{gen}}{k} \quad \textbf{...(4.8)}$$

$$T = -\frac{\dot{Q}_{gen}}{4k}r^2 + C_1 lnr + C_2 \quad \textbf{...(4.9)}$$

At r=0 -> $C_1 = 0$ and $r = R \rightarrow C_2 = T_0$

$$T = T_0 + \frac{\dot{Q}_{gen}}{4k}(R^2 - r^2) \quad \textbf{...(4.10)}$$

4.3.2 Solving homogenous part by the method of separation of variable

$$T(r,t) = G(r).S(t) \quad \textbf{...(4.11)}$$

$$\frac{1}{G}\frac{\partial}{\partial r}\left(r\frac{\partial G}{\partial r}\right) = \frac{\rho C_p}{kS}\frac{\partial S}{\partial t} = -\lambda^2 \quad \textbf{...(4.12)}$$

Solving for $G(r)$

In general Bessel Function is of the form

$$\mathrm{r}^2.\frac{\mathrm{d}^2\mathrm{G}}{\mathrm{dr}^2} + \mathrm{r}.\frac{\mathrm{dG}}{\mathrm{dr}} + (\lambda^2 - \mathrm{n}^2)\mathrm{r} = 0$$

$$\mathrm{r}^2\frac{\mathrm{d}^2\mathrm{G}}{\mathrm{dr}^2} + \mathrm{r}\frac{\mathrm{dG}}{\mathrm{dr}} + \lambda^2\mathrm{r}^2\mathrm{G} = 0 \qquad \text{Here n=0} \qquad \textbf{...(4.13)}$$

$$G(r) = C_1 J_0(\lambda r) + C_2 Y_0(\lambda r) \quad \textbf{...(4.14)}$$

$$G(R) = T_0 \; i.e. \; J_0(\lambda_k) = T_0 \quad \textbf{...(4.15)}$$

Where $\lambda_k = \frac{\alpha_0 k}{R^2} = \lambda^2$;

Solving for S(r):

$$\frac{dS}{dt} = -\frac{\lambda_k k}{\rho c_p} S \quad \textbf{...(4.16)}$$

$$S_k(t) = e^{-\frac{\lambda_k k}{\rho c_p}}$$

Combining these two equations;

$$T(r,t) = T_0 + \frac{\dot{Q}_{gen} R^2}{4k}\left[1 - \frac{r^2}{R^2} + \sum_{k=1}^{\infty} a_k J_0\left(\frac{\lambda_k r}{R}\right) e^{-\frac{\lambda_k k}{\rho c_p} t}\right] \quad \textbf{...(4.17)}$$

Normalizing the solution:

$$\boldsymbol{T(r,t) = T_0 + \frac{\dot{Q}_{gen} R^2}{4k}\left[\sum_{k=1}^{\infty} \frac{8k}{\lambda_k^3 J_1(\lambda_k)} J_0\left(\frac{\lambda_k r}{R}\right)\left(1 - e^{-\frac{\lambda_k k}{\rho c_p} t}\right)\right]} \quad \textbf{...(4.18)}$$

By using computational software, we can find temperature along the radial profile.

4.4 CONJUGATE HEAT TRANSFER FUNDAMENTALS

Conjugate heat transfer corresponds to heat transfer between solids and liquids through their interface. Generally, in solids conduction mode of heat transfer dominates and depending on parameters convection or conduction will dominate in fluids. In the case of cell and coolant fluid heat transfer from the center of the cell is carried to cell surface through conduction and from interface to fluid through convective heat transfer alongside conduction. The conjugate heat transfer problems got credibility with the advent of computational software because of their tedious calculations.

Certain assumptions are made in the simulation for the purpose of reducing complexities in the problem. They are,

- Heat is assumed to be generated at the center of the cell and gets distributed along the radial direction.
- The region of analysis is hydrodynamically forming region, thus the flow is turbulent.
- There is a physical separator of negligible thickness between the outer cell surface and fluid to separate direct contact. Its effect is neglected and analysis is done by assuming as if it is absent.

The heat flow in the cell is given by following partial differential equation.

$$\nabla \cdot (k\nabla T) + \dot{Q}_{gen} = \rho c_p \frac{\partial T}{\partial t} \quad \textbf{...(4.19)}$$

For homogenous isotropic materials we can assume thermal conductivity k to be constant and we can rewrite the above equation as

$$\nabla^2 T + \dot{Q}_{gen} = \frac{1}{\alpha}\frac{\partial T}{\partial t} \quad \textbf{...(4.20)}$$

In fluids heat transfer is quite complicated. There are three major contributors to the heat equation. During the transport of fluid, there is also a transfer of energy this appears as convective heat transfer. The second effect is the viscous effects of fluid flow causes heating of fluid similar to friction causing heating of the object due to the dissipation of energy. This is neglected for low velocities but becomes an important factor for high velocity flows. The last contribution is due to the fact that density is temperature dependent thus a pressure work term contributes to the heat equation since the pressure is related to the density of the fluid. Thus the governing differential equation can be written as-

$$\rho c_p \frac{\partial T}{\partial t} + \rho c_p \boldsymbol{u} \cdot \nabla T = \alpha_p T \left(\frac{\partial p_f}{\partial t} + \boldsymbol{u} \cdot \nabla p_a\right) + \tau : S + \nabla \cdot (k\nabla T) + \dot{Q}_{gen} \quad \textbf{...(4.21)}$$

The temperature field and the heat flux are continuous at the fluid-solid interface. In the interior part of solid depending on transient or steady state temperature can be varying or constant. But the temperature in the fluid can vary in different regions irrespective of transient and steady-state nature. At interface fluid

temperature is the same as that of interface temperature; far from the interface, it is close to ambient temperature. The boundary layer is the region where the fluid temperature is the same as that of interface temperature. Prandtl number (Pr)decides the extent of boundary layer thickness. For $Pr = 1$, thermal and momentum layer thickness need to be same and for $Pr > 1$ a thick momentum layer exists and for $Pr < 1$ thin momentum layer exists.

The dominance of convective and conductive mode of heat transfer depends on a parameter called Rayleigh number. It characterizes flow regime induced by the natural convection and the resulting heat transfer. Rayleigh number is given by-

$$Ra = \frac{\rho^2 g \alpha_p c_p \Delta T L^3}{\mu k} \quad \textbf{...(4.22)}$$

If Ra$< 10^{-3}$ natural convection and corresponding heat transfer can be neglected without much trouble. Another parameter which characterizes natural convection is Grashoff's number which is given by -

$$Gr = \frac{\rho^2 g \alpha_p \Delta T L^3}{\mu^2} \quad \textbf{...(4.23)}$$

These two numbers are connected by Prandtl's number as follows

$$Ra = Pr \cdot Gr \quad \textbf{...(4.24)}$$

The nature of flow i.e. laminar or turbulence is decided by buoyancy and viscous force. When buoyancy is greater compared to viscous effects the flow will be turbulent else it will be laminar. These two regimes of flow can be differentiable by critical order of Grashoff's number Flow is turbulent if $Gr \geq 10^9$ else it is laminar. We can find the overall heat transfer coefficient h; using the relation between Grashoff's, Prandtl's and Nuseelt's number given by-

$$Nu = C.Gr^n Pr^m \quad \textbf{...(4.25)}$$

where constants m and n are evaluated corresponding to the nature of the flow. The thickness of the boundary layer is given by-

$$\delta_{T_n} = \frac{L}{\sqrt[4]{Ra}} \quad \textbf{...(4.26)}$$

Forced convection is governed by another dimensionless parameter called Reynolds number which is the ratio of inertia force to viscous force. In this case flow regime is similar to isothermal flow because fluid at constant temperature flows constantly. We can find the overall heat transfer coefficient h; using the relation between Reynold's, Prandtl's and Nusselt's number given by:

$$Nu = C.Re^{n}Pr^{\frac{1}{3}} \quad \textbf{...(4.27)}$$

where constants are evaluated according to the nature of the flow. The thickness of the boundary layer is given by:

$$\boldsymbol{\delta_{T_f}} = \frac{\boldsymbol{L}}{\sqrt{\boldsymbol{Re}}} \quad \textbf{...(4.28)}$$

4.5 HEAT TRANSFER FROM SURFACE TO COOLANT FLUID

Heat transferred from surface to the coolant fluid, in a given time are found thus finding values of surface temperature and coolant fluid. In calculation, the resistance offered by metallic separator is neglected. It is assumed that heat transferred from four quarters of the cylinder is equivalent to heat transferred by one cell. The coolant inside the duct receives this heat energy and its temperature changes in subsequent time.

$$\text{Area of Duct} = d^2 - \frac{\pi}{4}d^2 \quad \textbf{...(4.29)}$$

Effective Diameter=Hydraulic Diameter $D_H = D = \frac{4A_c}{P}$ **...(4.30)**

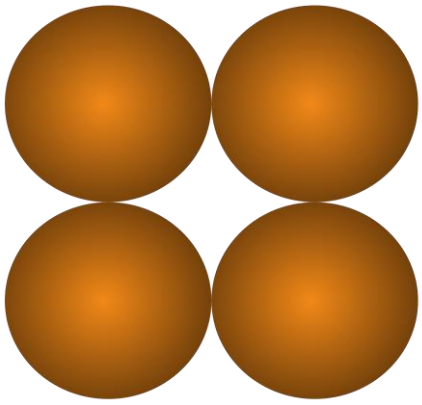

Figure 4.3 : Plane View of the cell pack

The **Figure 4.3** shows the plane view of the duct that is formed by four adjacent Lithium-ion cells. Thus, the area of duct formed is equal to the area of the fluid entry region. The fluid enters through a duct from one side and exits from other carrying away heat along its path. Fluid friction, turbulence effects, boundary layer formation is neglected in the study. The region is within hydro dynamically developing region.

There are two possible ways in which fluid flows. In one method fluid is made to flow continuously i.e. dynamic model and another one in which fluid is made to flow only in intervals when the fluid reaches a certain temperature in duct thus saving pumping power.

4.5.1 Dynamic Model

Here Reynolds number plays a significant role and is used to find the overall heat transfer coefficient. The model should obey the momentum equation, the continuity equation, and the energy equation.

$$Nu = C.Re^{m}.Pr^{\frac{1}{3}} \quad \textbf{...(4.31)}$$

For Reynolds number between 40.0 to 4000, we have C=0.683 and m=0.466

$$Nu = 0.683.Re^{0.466}.Pr^{\frac{1}{3}} \quad \textbf{...(4.32)}$$

$$\frac{\partial}{\partial t}\left(\rho_f \vec{v}\right) + \nabla.\left(\rho_f \langle \vec{v}|\vec{v}\rangle\right) = -\nabla\vec{p}\ ; \text{ Momentum Equation} \quad \textbf{...(4.33)}$$

$$\frac{\partial}{\partial t}\left(\rho_f C_{pf} T_f\right) + \nabla.\left(\rho_f C_{pf} T_f\right) = -\nabla.\left(\mathrm{k_g}\nabla T_g\right)\ ; \text{ Energy Equation} \quad \textbf{...(4.34)}$$

$$\frac{\partial}{\partial t}\left(\rho_f \vec{v}\right) + \nabla.\left(\rho_f \vec{v}\right) = 0\ ; \text{ Continuity equation} \quad \textbf{...(4.35)}$$

$$h = \frac{k}{D}0.683.Re^{0.466}.Pr^{\frac{1}{3}} \quad \textbf{...(4.36)}$$

$$Q = h.A_s.\left(T_s - T_{f0}\right) = -\dot{m}.t.C_{pf}.\frac{dT}{dt} \quad \textbf{...(4.37)}$$

Here T_s is constant for the first iteration and it gets updated for subsequent iterations. Thus, the final equation

$$\ln(t) = \frac{mC_{pf}}{hA}\ln\left[\frac{T_s - T_{f0}}{T_s - T_{f1}}\right] \quad \textbf{...(4.38)}$$

The parameters and their values are given in **Table 4.1** below.

Parameter	Value
Prandtl Number; Pr	0.701
Density of air; ρ_{air}	1.165 kg/m^3
Thermal conductivity of air; k_{air}	0.02675 W/mK
Specific heat capacity of the air; c_p	1005 J/kg
Dynamic Viscosity of air; μ	18.63×10^{-6}
Area of Conduit;D_h	69.53×10^{-6}
Air Velocity; v_{air}	0.25m/s

Table 4.1 : Parameters and their value

4.5.2 Static Model

Here natural convection is considered, fluid is replaced only after certain time interval i.e. when it reaches threshold temperature.

Determining overall heat transfer coefficient,

Grashoff's number,

$$Gr = \frac{D^3 g \beta \Delta t}{\nu^2} \quad \textbf{...(4.39)}$$

Mc-Adams Correlation:

$$Nu = \begin{Bmatrix} 0.59(Gr.Pr)^{0.25}, & for\ laminar\ flow\ Gr.Pr < 10^9 \\ 0.10(Gr.Pr)^{\frac{1}{3}}, & for\ turbulent\ flow\ 10^9 < Gr.Pr < 10^{12} \end{Bmatrix}$$

$$\beta = \frac{1}{\rho}\left(\frac{\partial p}{\partial T}\right)_p \quad \textbf{...(4.40)}$$

$$h = \frac{k}{D} 0.59(Gr.Pr)^{0.25} \quad \textbf{...(4.41)}$$

$$Q = h.A_s.\left(T_s - T_{f0}\right) = -mC_{pf}\frac{dT}{dt} \quad \textbf{...(4.42)}$$

Here T_s is constant for the first iteration and it gets updated for subsequent iterations; $T_f \ varies \ as \ T_{fo} \ T_{f1} \ T_{f2}$ for further iterations. Thus, the final equation is

$$t = \frac{mC_{pf}}{hA_s} \ln \left[\frac{T_s - T_{f0}}{T_s - T_{f1}} \right] \qquad \textbf{...(4.43)}$$

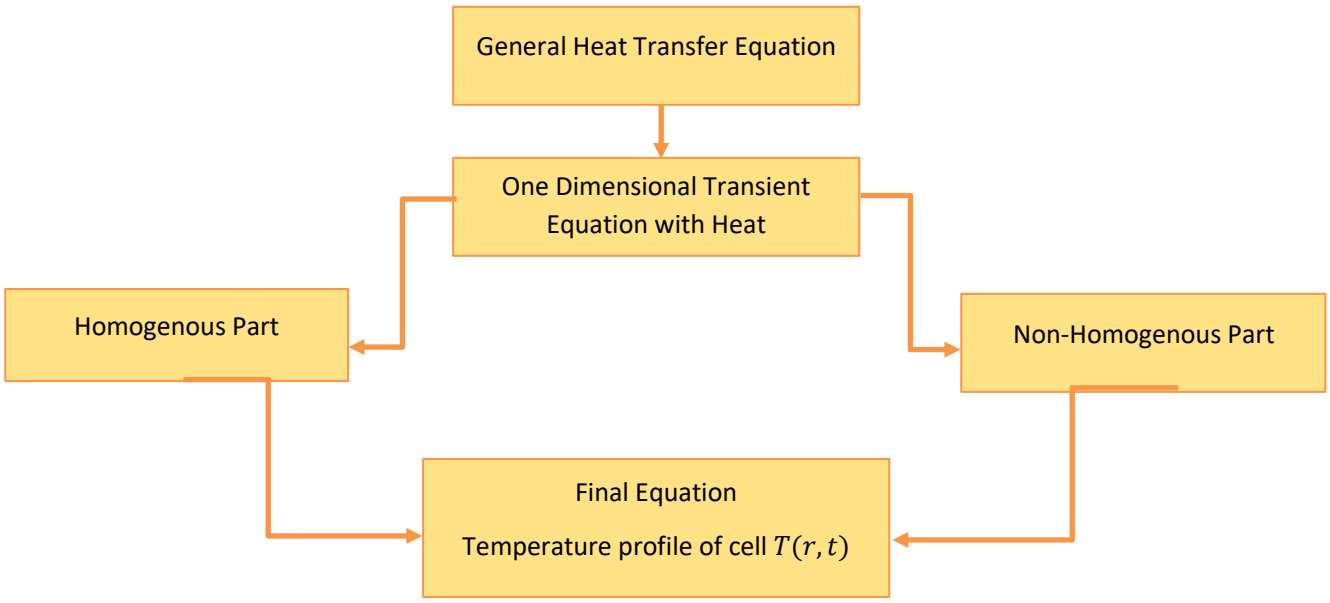

Figure 4.4 : The mathematical modelling expressed in the form of a flowchart

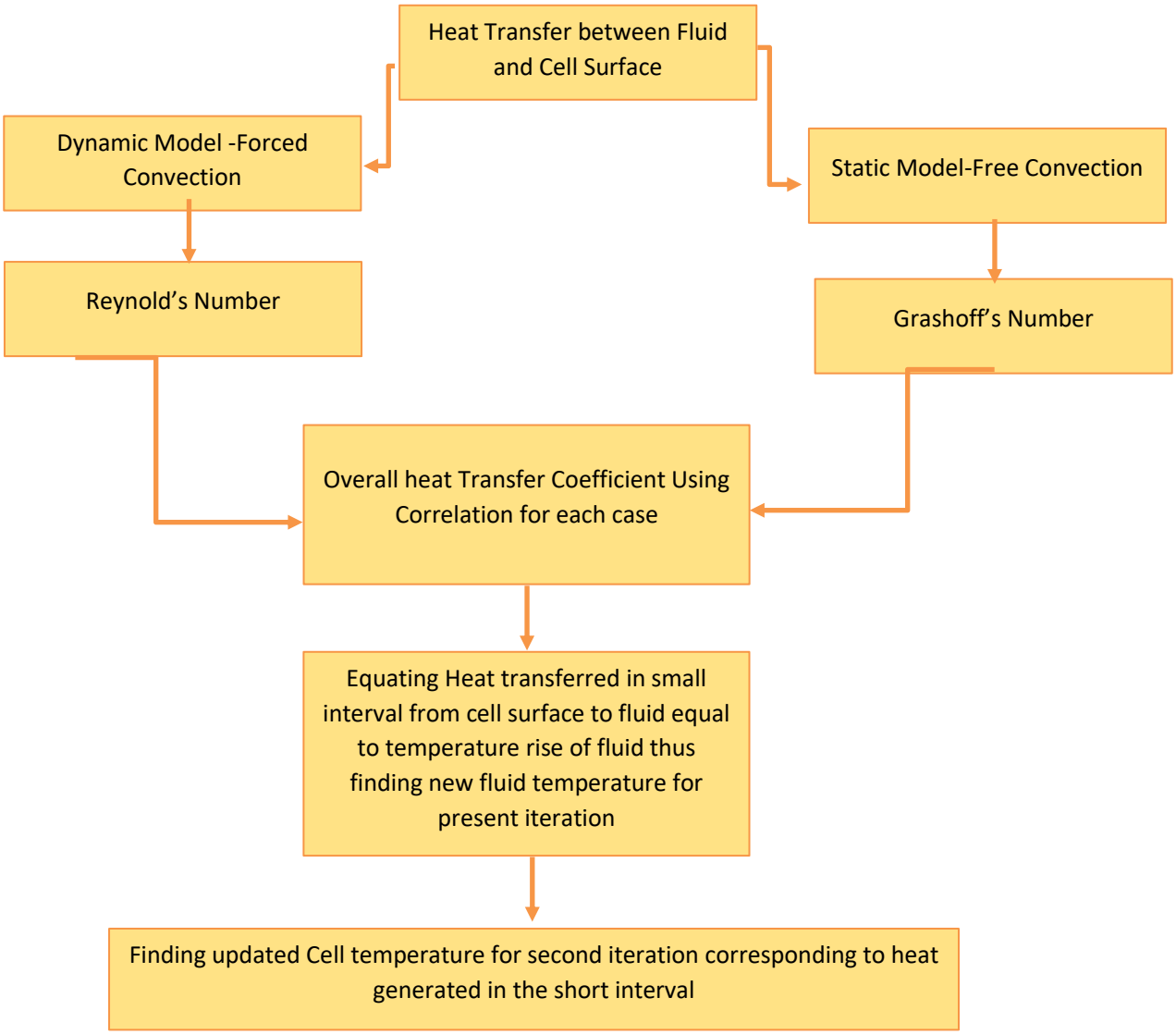

Figure 4.5 : Heat Transfer between Fluid and Cell Surface

4.6 INTRODUCTION TO NANOFLUIDS

A nanofluid is a fluid containing nanometre-sized particles called nanoparticles. These fluids are engineered colloidal suspensions of nanoparticles in a base fluid. The nanoparticles used in nanofluids are typically made of metals, oxides, carbides, or carbon nanotubes. Common base fluids include water, ethylene glycol, and oil. They exhibit enhanced thermal conductivity and the convective heat transfer coefficient compared to the base fluid.

4.7 SYNTHESIS OF NANOFLUID

- A certain amount of Nano-particles (Al_2O_3) are dispersed in base fluid like water, ethylene glycol or other engine oils by Ultrasonication process**.**
- Ultrasonication is a process that uses sound energy at high frequencies to break apart particle agglomerates by cavitation, the expansion, and implosion of bubbles.

4.8 CORRELATIONS FOR NANOFLUID

- Density $\rho_{nf} = \phi\rho_p + (1-\phi)\rho_f$ **…(4.44)**
- Specific Heat: $(\rho c_p)_{nf} = \phi(\rho c_p)_p + (1-\phi)(\rho c_p)_f$ **…(4.45)**
- Viscosity $\mu_{nf} = \mu_f(1-\phi)^{2.5}$ **…(4.46)**
- Prandtl Number $Pr = \frac{\mu c_p}{k}$ **…(4.47)**
- Enthalpy/Heat of Formation $\Delta h_f = \phi\Delta h_{f_p} + (1-\phi)\Delta h_{f_f}$ **…(4.48)**
- Thermal Conductivity $k_{nf} = \frac{k_p+2k_f-2\phi(k_f-k_p)}{k_p+2k_f+\phi(k_f-k_p)}\ k_f$ **…(4.49)**
- Gram Molecular Mass: GMM =$\phi M_p + (1-\phi)M_f$ **…(4.50)**
- Thermal Expansion $(\beta\rho)_{nf} = \phi(\beta\rho)_p + (1-\phi)(\beta\rho)_f$ **…(4.51)**

Chapter 5

Methodology

CHAPTER 5

METHODOLOGY

5.1 INTRODUCTION TO SIMSCALE

SimScale is a computer aided engineering (CAE) software product based on cloud computing. SimScale was developed by SimScale GmbH and allows Computational Fluid Dynamics, Finite Element Analysis and Thermal simulations.[12][13] The backend of the platform uses open-source codes:

- CFD: OpenFOAM

The cloud-based platform of SimScale allows users to run more simulations, and in turn iterate more design changes, compared to traditional local computer-based systems.[14]

The stages of analysis using SimScale involves Pre-processing, Simulation, and Post-processing.

5.2 PRE-PROCESSING

The pre-processing stage involves importing a file and meshing.

The file formats supported by SimScale are

- STEP
- IGES
- BREP
- STL

STEP is the preferred one since it's superior in terms of the conversion process to IGES. The STL format can only be used for fluid mechanics analysis since only certain meshing algorithms on SimScale support i

To run a fluid mechanics simulation, you have to provide the actual fluid volume. For internal fluid flow analyses, this means that you have to extract the region in your CAD model as a single part and upload this part to SimScale. Often this means that you have to invert your CAD assembly to identify where the fluid actually flows.

5.2.1 Meshing

SimScale platform offers various meshing capabilities to create computational grids. Several algorithms are available for users to create three-dimensional tetrahedral and hexahedral meshes on the platform. Due to robustness and general applicability of applied algorithms, both automated and manual versions of these meshing algorithms are provided.

Current meshing strategies available on the platform are:

- Tet-dominant
- Hex-dominant automatic (only CFD)
- Hex-dominant automatic “wind-tunnel/external flow” (only CFD)
- Hex-dominant parametric (only CFD)

5.3 SIMULATION

The analysis type **Conjugate heat transfer (CHT)** allows the simulation of the heat transfer between **Solid** and **Fluid** domains by exchanging thermal energy at the interfaces between them. It requires a **multi-region** mesh to have a clear definition of the interfaces in the computational domain. Such a mesh can be created with the **Hex-dominant parametric** operation in the mesh creator.

5.3.1 Turbulence Model

A turbulence model should be chosen in accordance to the flow regime. In a Laminar flow, associated with low Reynolds numbers, viscous effects dominate the flow and turbulence can be neglected. This flow regime is characterized by regular flow layers.

On the other hand, a Turbulent flow is characterized by chaotic and irregular patterns that are associated with high Reynolds numbers. In order to simulate turbulent fluid flow, an appropriate turbulence model should be chosen. Currently, these models are supported:

- Laminar
- Reynolds-Averaged Navier–Stokes (RANS)
    - k-Epsilon
    - kOmega-SST
- Large eddy simulation (LES)
    - Smagorinsky

5.3.2 Solver

The conjugate heat transfer simulations use the following OpenFOAM solvers:

- **chtMultiRegionFoam**.

For transient simulations with laminar or turbulent flow. This solver uses the PIMPLE method for iterative solution.

- **chtMultiRegionSimpleFoam**.

For Steady State simulations with laminar or turbulent flow. This solver uses the SIMPLE method for iterative solution.

5.4 POST-PROCESSING

The temperature contours are obtained from SimScale and the further post-processing is performed by importing the results to ParaView.

5.5 SIMULATION METHODOLOGY

The numerical simulation for the electrochemical model was performed by means of Simscale, an opensource cloud-based software for FEA, CFD and thermal simulations. The simulations were carried out for multicell arrangement.

5.6 MULTICELL SIMULATION

The sequence of events followed for the simulation of multicell arrangements are as mentioned below:

- A 3D model of the Lithium-ion 18650 cells (4x4 grid) placed inside a specialized casing consisting of mini-channels was created using CATIA V5 which was imported to the Simscale workbench.
- Conjugate Heat Transfer (CHT) simulation was selected to analyze the cooling of the multicell arrangement by using different cooling fluids.
- The 3D model was meshed using the hex-dominant parametric algorithm with an additional surface mesh refinement given to the cell surfaces.
- The surrounding temperature, the inlet cooling fluid temperature and the cell initial temperature were all set as $27^{o}C$.
- Mass flow rate and outlet pressure (atmospheric pressure) were selected as the inlet and outlet boundary conditions.
- The walls between flow region and solid region, and between different solid regions were set as thermally coupled walls.
- Discharge rate of the cells and mass flow rate of the cooling fluid were varied to give in total 12 different cases for a single cooling fluid:
    1. Discharge rates
        a). 1C
        b). 2C
        c). 3C

2. Mass flow rates
    a). 0.01m/s
    b). 0.1m/s
    c). 0.5m/s
    d). 1m/s

- No slip shear condition and stationary wall were applied to the mini-channels.
- The laminar model was selected because the Reynolds number was less than 2300 for different mass flow rates considered.
- Time step is taken as 1 second for more accuracy and 10 write intervals were taken in order to have sufficient data for post-processing.
- Cooling fluids considered for simulation:
    1. Air
    2. Water
    3. Water + Ethylene Glycol mixture
    4. Water + 1%Al_2O_3
- **Varied Parameters are**:

1. Coolant Fluid:

a) Air
b) Water
c) Water-Ethylene Glycol
d) Water+Al_2O_3

2. Discharge Rate:

a) 1C – 0.0896W; 3600s
b) 2C – 0.5248W; 2400s
c) 3C – 1.0284W 1200s

3. Flow Velocity:

a) 0.01m/s
b) 0.05 m/s
c) 0.5 m/s

d) 1m/s

- The various properties of these cooling fluids are given in the **Table 8.1** below:

Property	**Air**	**Water**	**Water + Ethylene Glycol**	**Water + 1% Al_2O_3**
Molar mass (kg/kmol)	28.97	18	31.2	18.8396
Dynamic viscosity (kg/s.m)	0.0000183	0.000931297	0.00315	0.0008337
Prandtl number	0.713	6.5241	26.26	3.185
Specific heat (J/kg.K)	1004	4180	3494	4049.872
Heat of formation (J/kg)	0	-15878000	-10788.46154	-15908488

Table 5.1 : Cooling fluids and their properties

- The methodology is depicted in a flowchart below for easy understanding:

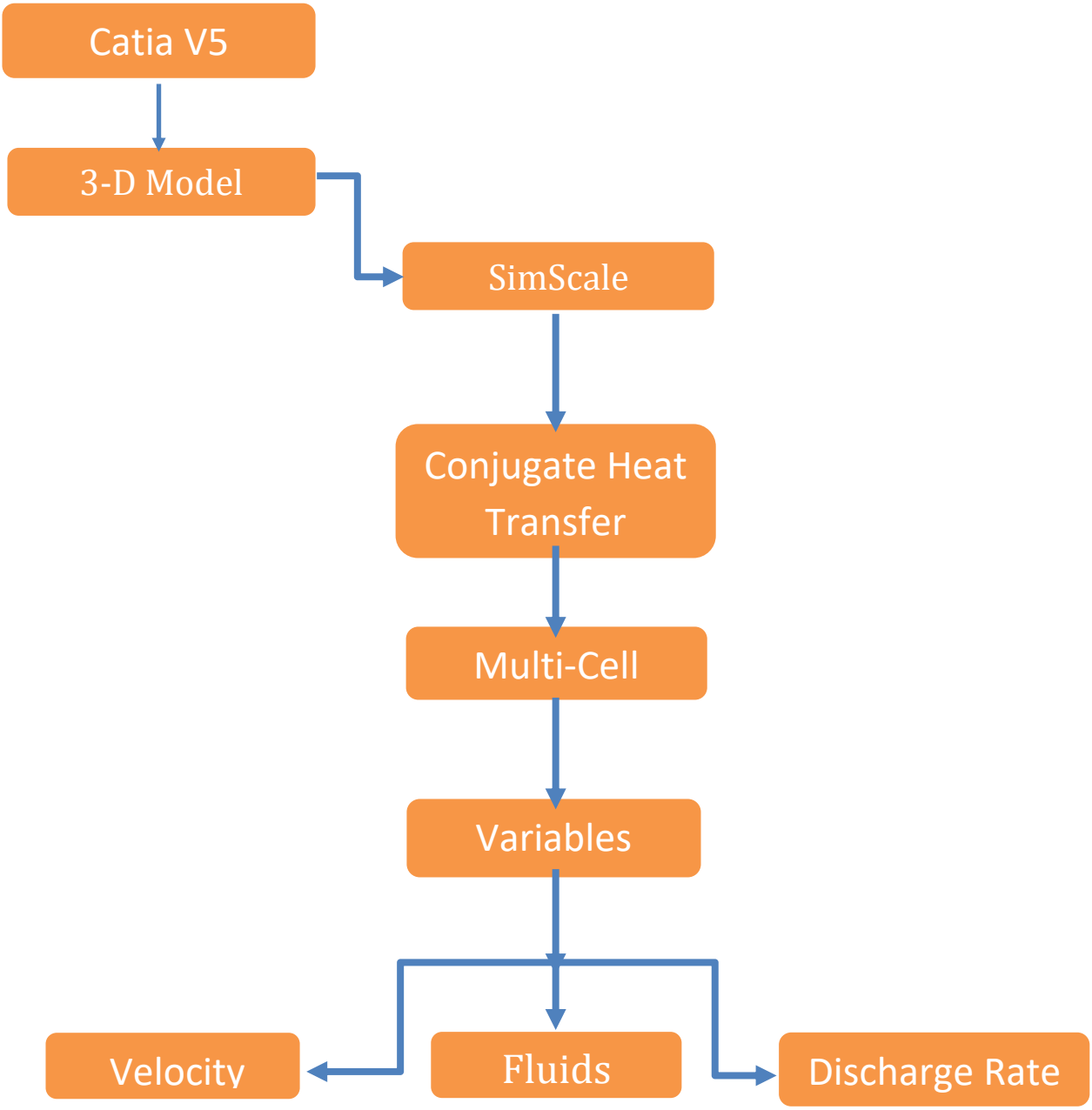

Figure 5.1 : Flowchart of the Simulation Methodology

Chapter 6

Results and Discussion

CHAPTER 6

RESULTS AND DISCUSSION

6.1 RESULTS

The simulated results while passing different cooling fluids at different flow rates and at different discharge rates of cell can be witnessed in this section. These simulated results can be compared with each other to know the efficiency of a certain cooling fluid in reducing the maximum temperature reached and thus increasing the life of a battery.

6.2 RESULTS WITH AIR AS COOLANT

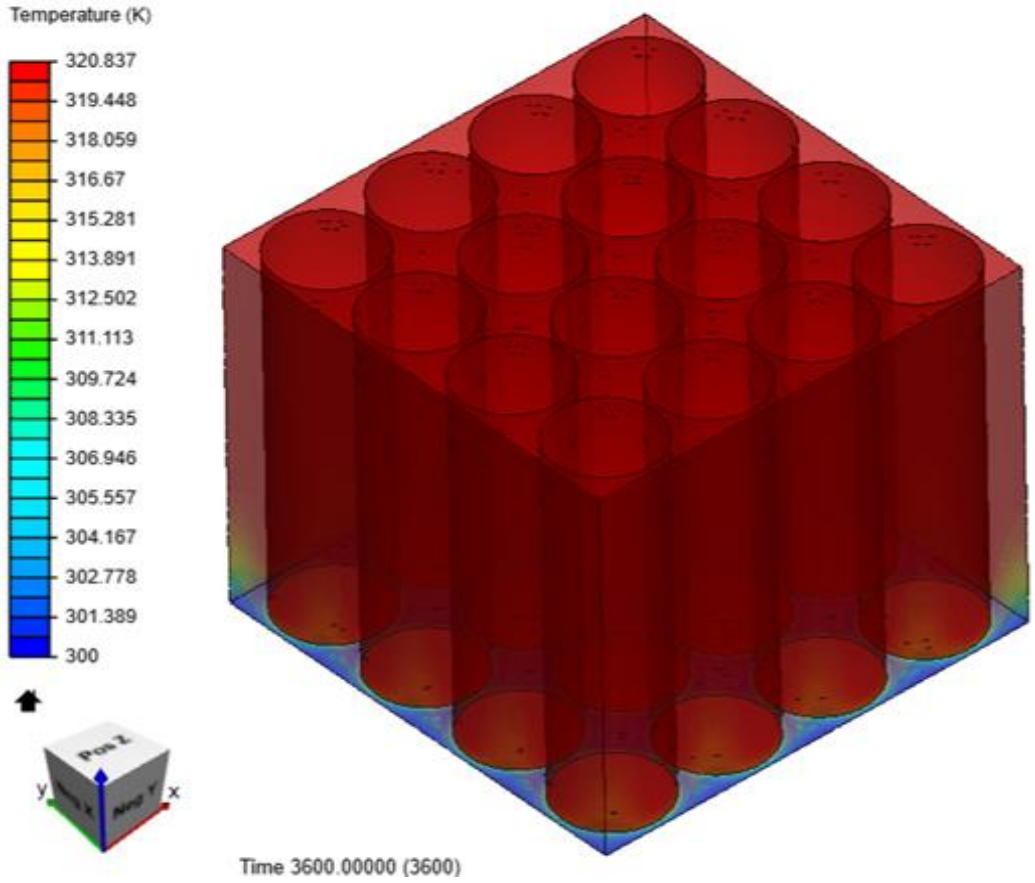

Figure 6.1 : Air with 0.01m/s velocity and 1C discharge rate

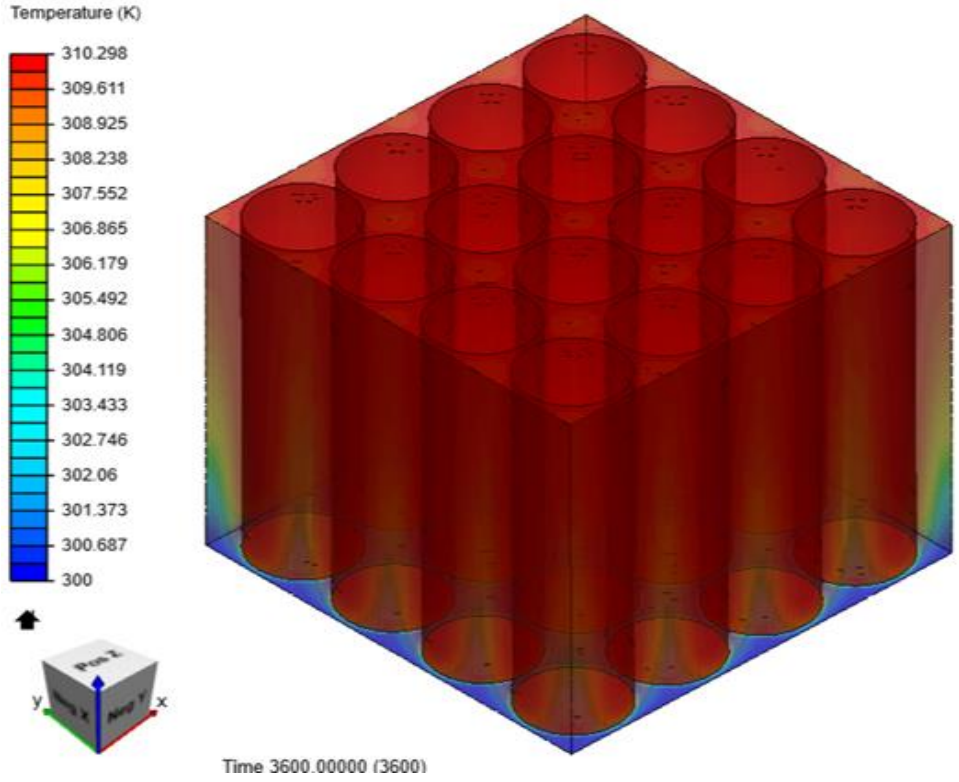

Figure 6.2 : Air with 0.05 m/s velocity and 1C discharge rate

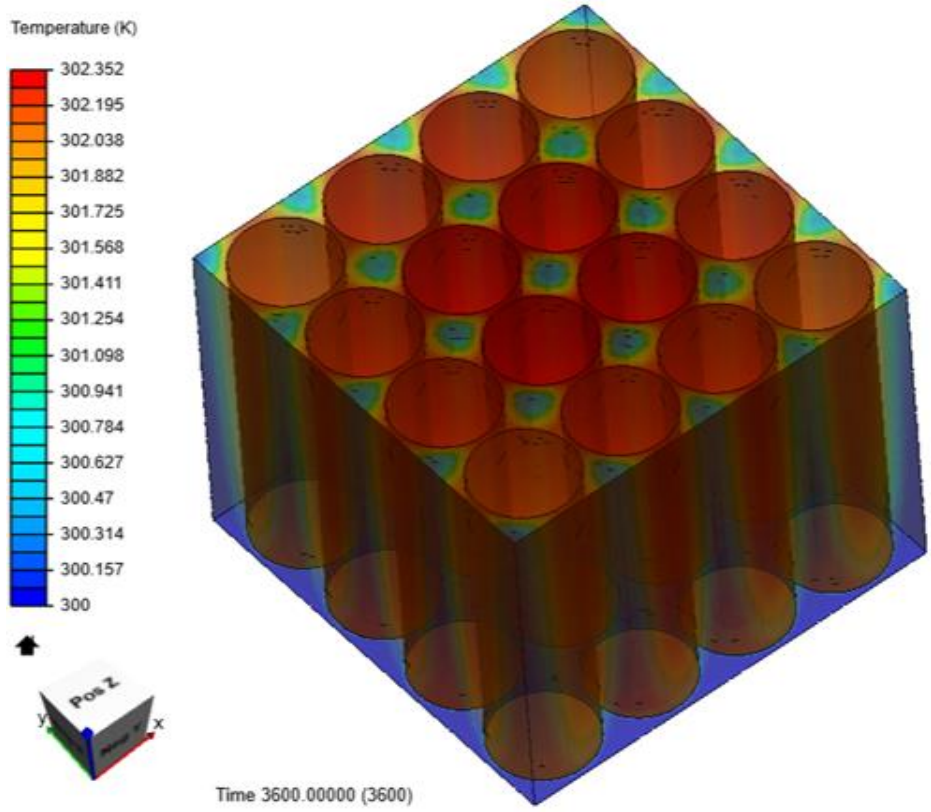

Figure 6.3 : Air with 0.5 m/s velocity and 1C discharge rate

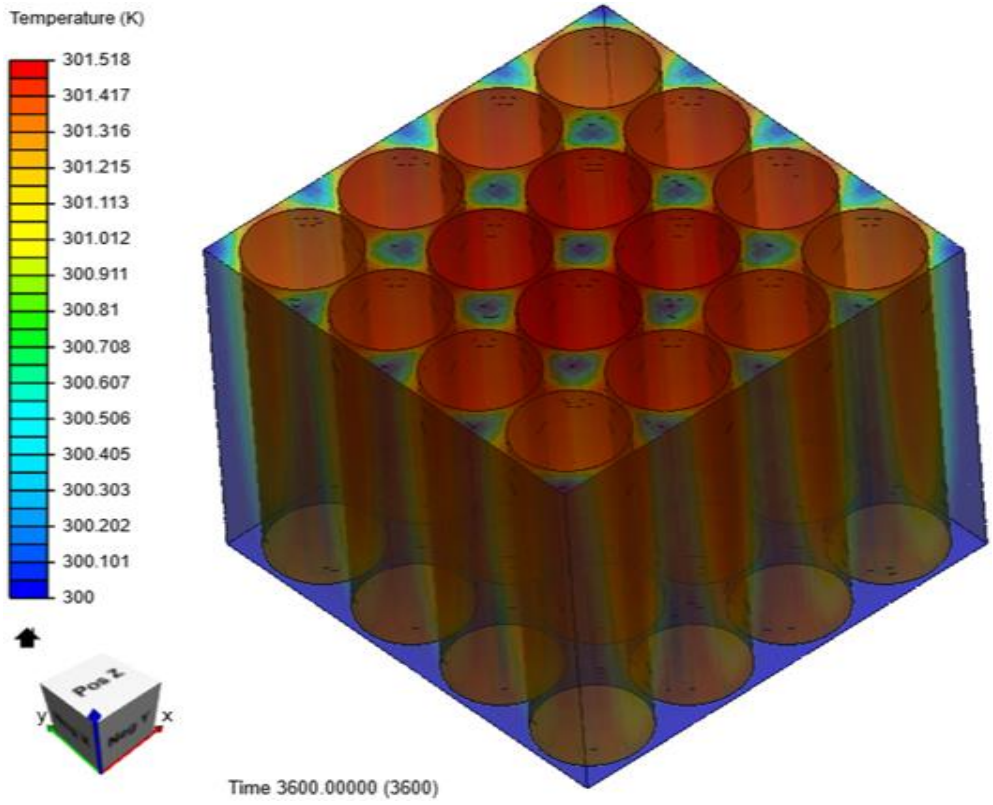

Figure 6.4 : Air with 1 m/s velocity and 1C discharge rate

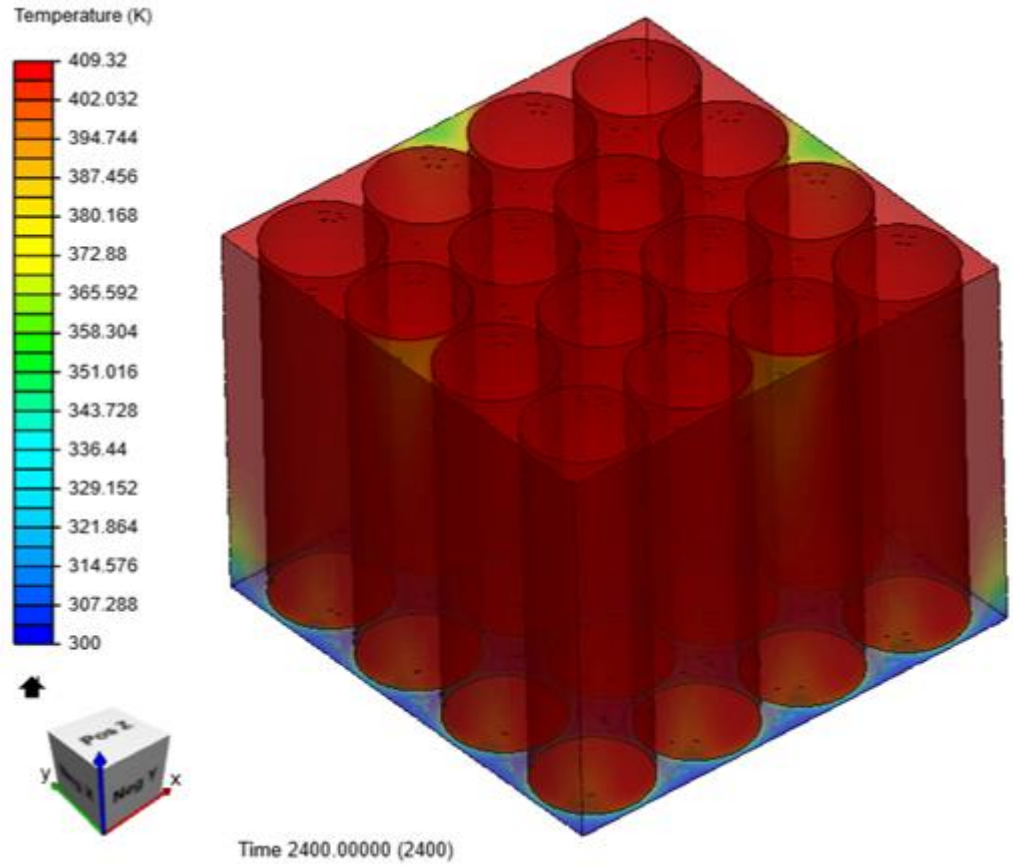

Figure 6.5 : Air with 0.01 m/s velocity and 2C discharge rate

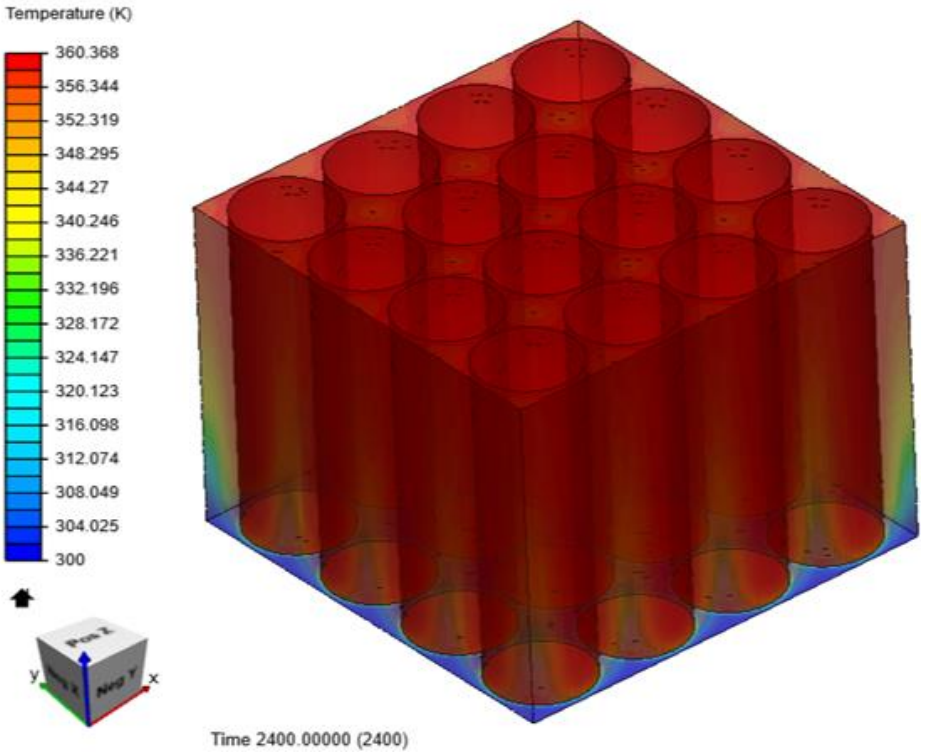

Figure 6.6 : Air with 0.05 m/s velocity and 2C discharge rate

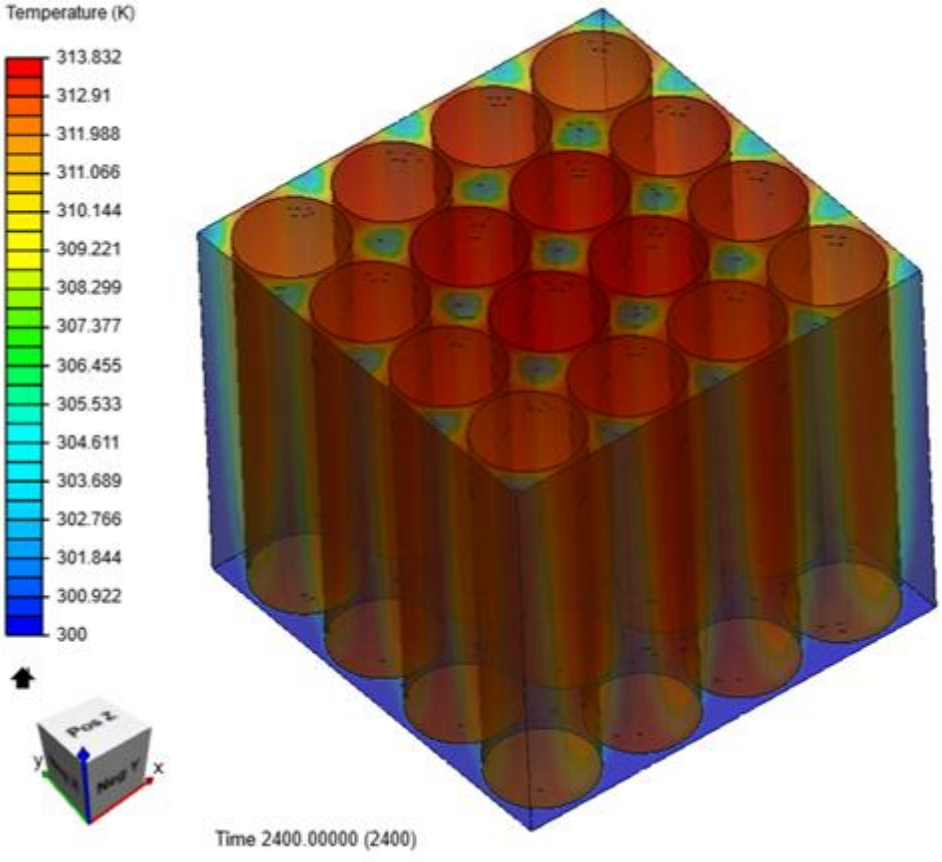

Figure 6.7 : Air with 0.5 m/s velocity and 2C discharge rate

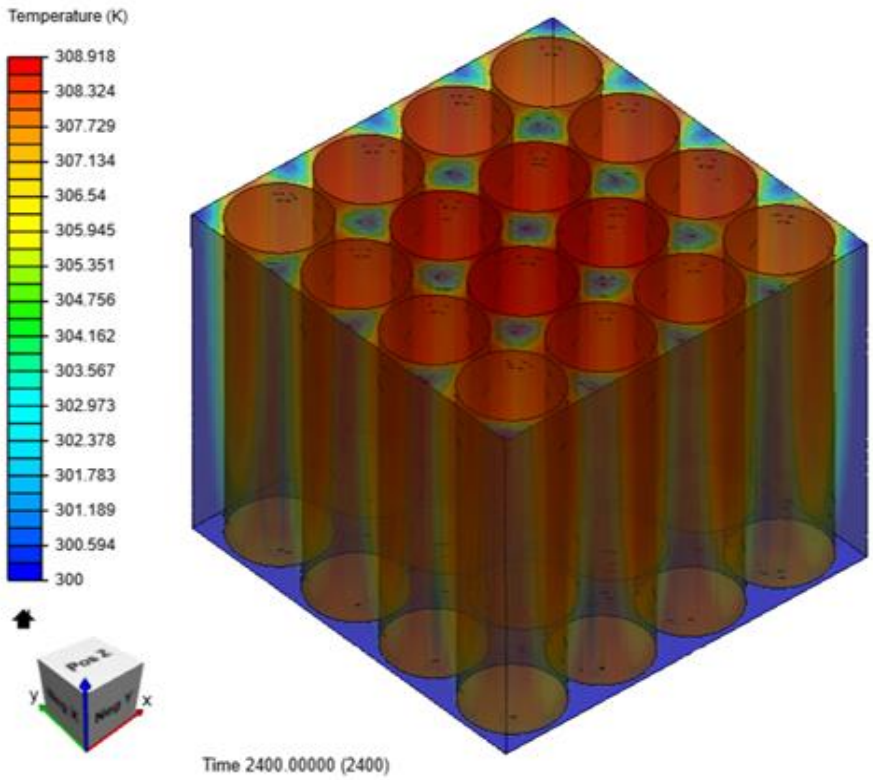

Figure 6.8 : Air with 1 m/s velocity and 2C discharge rate

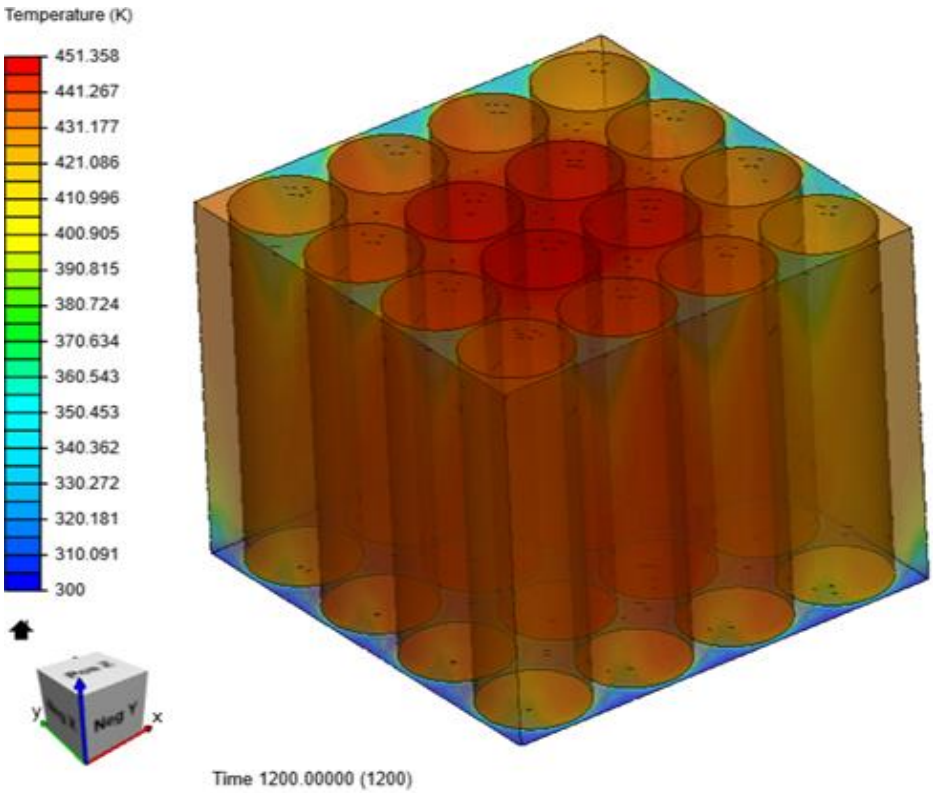

Figure 6.9 : Air with 0.01 m/s velocity and 3C discharge rate

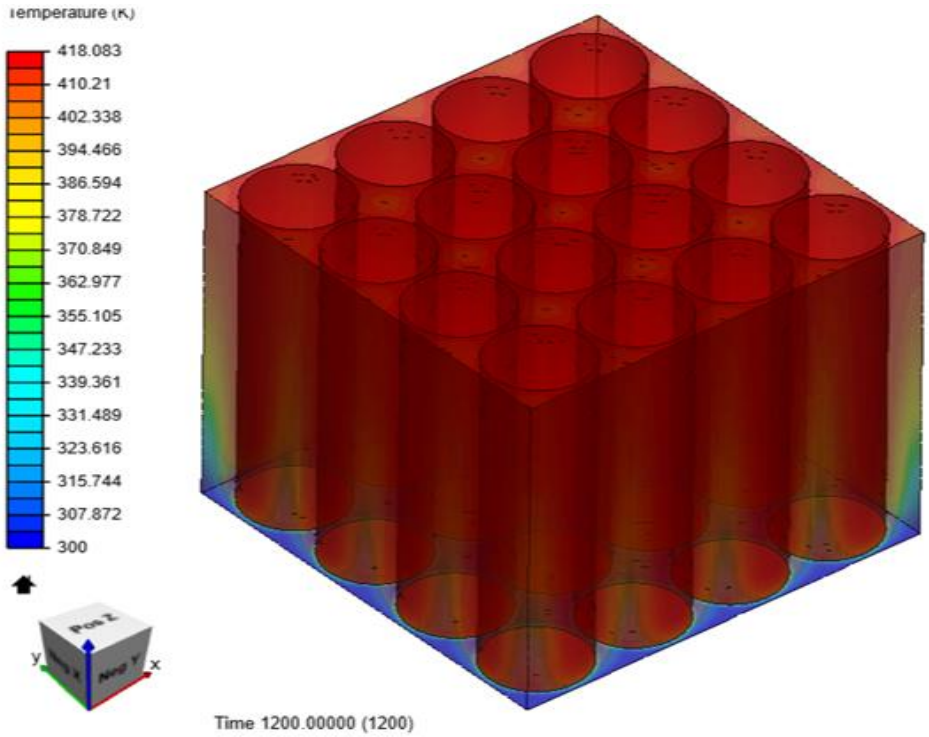

Figure 6.10 : Air with 0.05 m/s velocity and 3C discharge rate

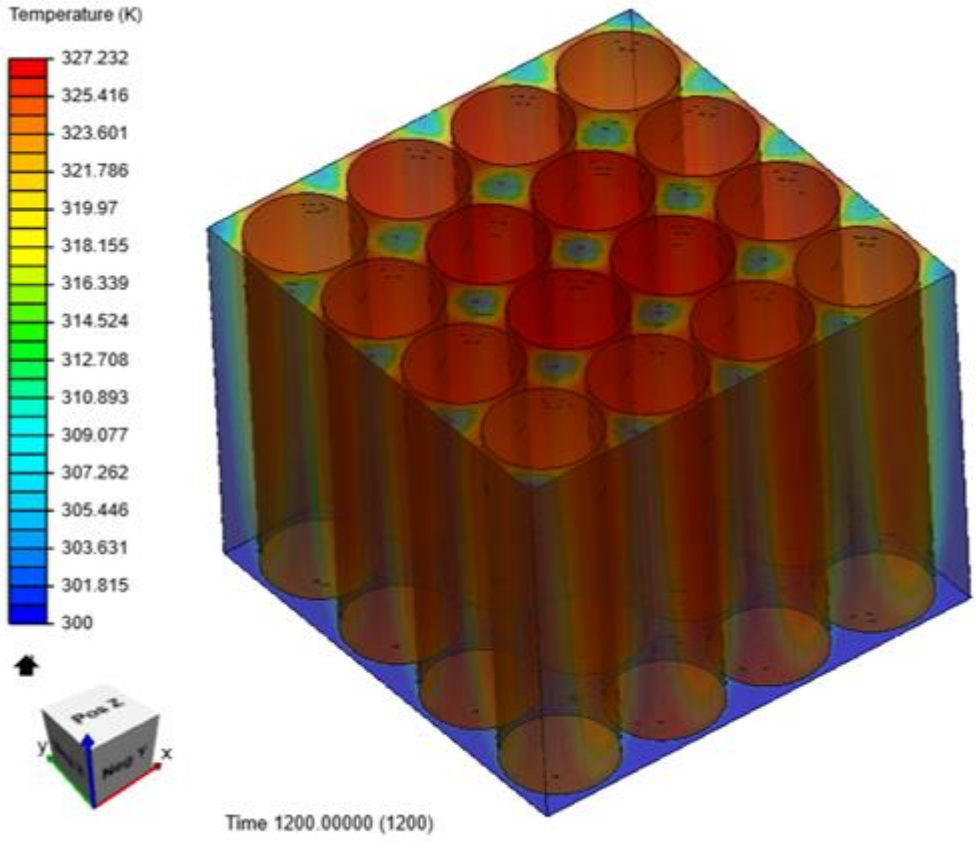

Figure 6.11 : Air with 0.5 m/s velocity and 3C discharge rate

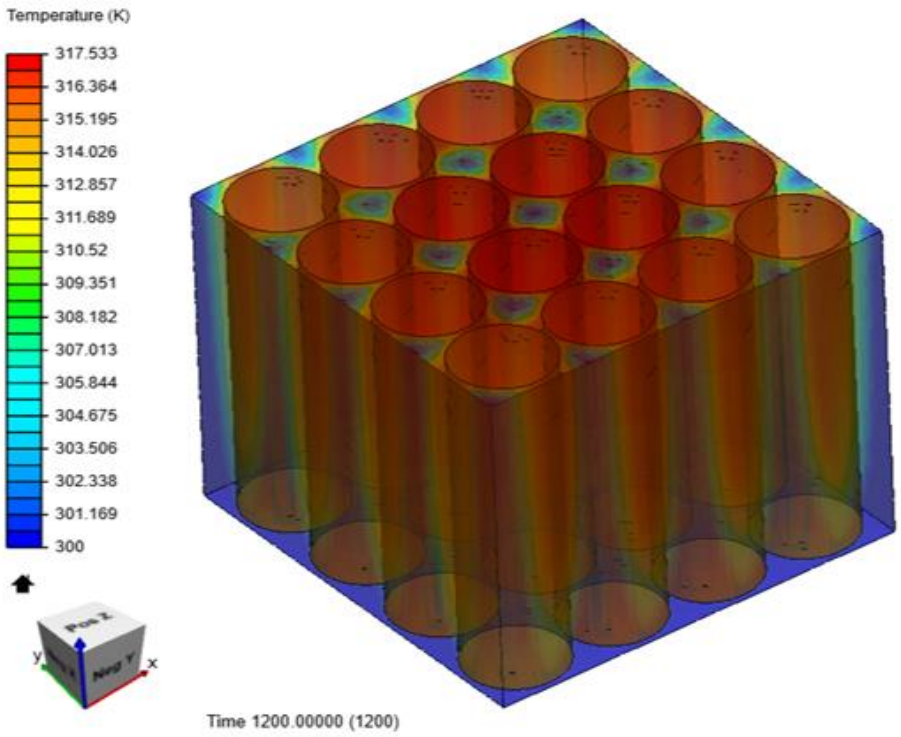

Figure 6.12 : Air with 1 m/s velocity and 3C discharge rate

6.3 DISCUSSION FOR AIR AS COOLANT

CASE	Inlet Velocity (m/s)	Discharge Rate (C)	Maximum Battery Pack Temperature (K)
1	0.01	1C	320.837
2	0.05	1C	310.298
3	0.5	1C	302.352
4	1	1C	301.518
5	0.01	2C	409.32
6	0.05	2C	360.368
7	0.5	2C	313.832
8	1	2C	308.918
9	0.01	3C	451.358
10	0.05	3C	418.083
11	0.5	3C	327.232
12	1	3C	317.533

Table 6.1 : Maximum temperature for various conditions for Air

The simulation is carried out first using Air as the cooling fluid, wherein the maximum battery pack temperature reaches around 321K.The low discharge rate of the cells and the low velocity air is able to limit the temperature from going into the thermal runaway region.

An increase of inlet velocity to 0.05m/s causes a decrement in the battery pack temperature by 10K.The cause of this decrease is the increase in the inlet velocity of the air, thereby allowing fresh fluid to flow through the ducts enhancing the heat transfer from cell to the air.

The inlet air velocity of 0.5m/s is able to bring down the temperature to 302K which is within the optimum range of the Lithium ion 18650 cell.

Further increase in the velocity of air leads to the battery pack temperature to decrease further down to 301.5K.

The discharge rate is varied to 2C (cell discharges 2Amp current continuously for an hour) which leads to an increment in heat generation hence an increase in maximum battery pack temperature to 409K for 0.01m/s inlet velocity of air and 360K for 0.05m/s inlet velocity of air. Such high temperatures will cause the thermal runaway of the Lithium ion cell. Hence for 2C discharge rate, with air as coolant and low inlet velocities are not sufficient to cool the battery pack.

With higher inlet velocities of air (0.5m/s and 1m/s) the battery pack temperature remains within the optimum working range.

The discharge rate of the cells is increased to 3C causing further increment in heat generation and increment in battery temperature to 451K and 418K for 0.01m/s and 0.05m/s inlet velocity of air respectively. These high temperatures will lead to failure of the battery pack; hence the inlet velocity is increased to 0.5m/s resulting in lowering of the battery temperature to 327K which is slightly above the optimum range. Therefore, the inlet velocity is further increased to 1m/s, thereby bringing down the maximum battery pack temperature to 317K.

6.4 RESULTS WITH WATER AS COOLANT

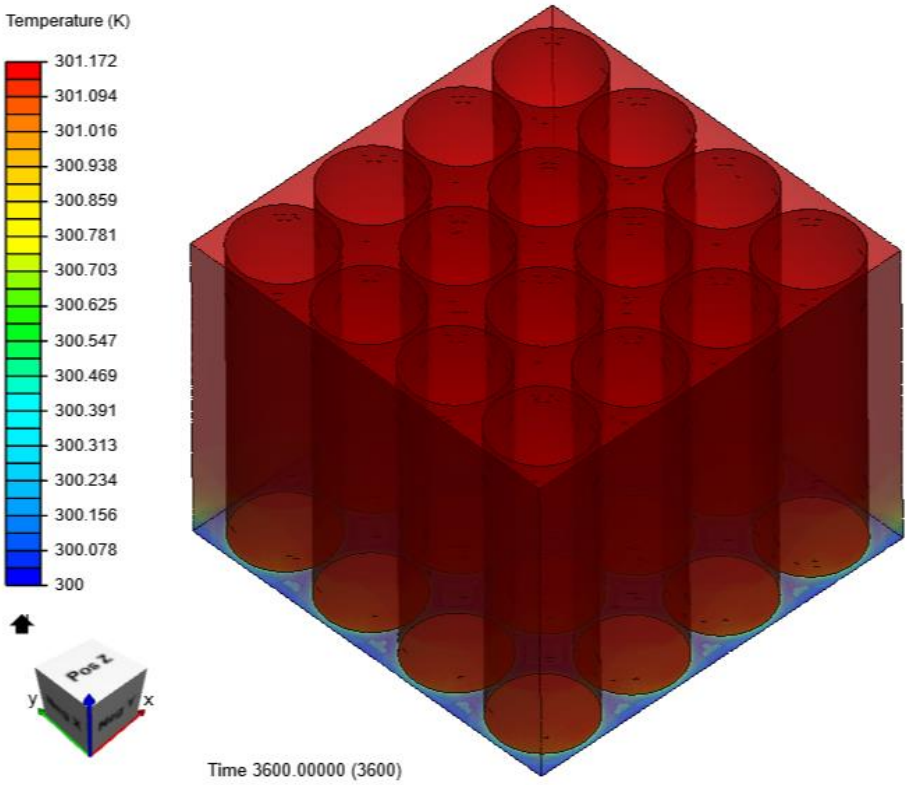

Figure 6.13 : Water with 0.01 m/s velocity and 1C discharge rate

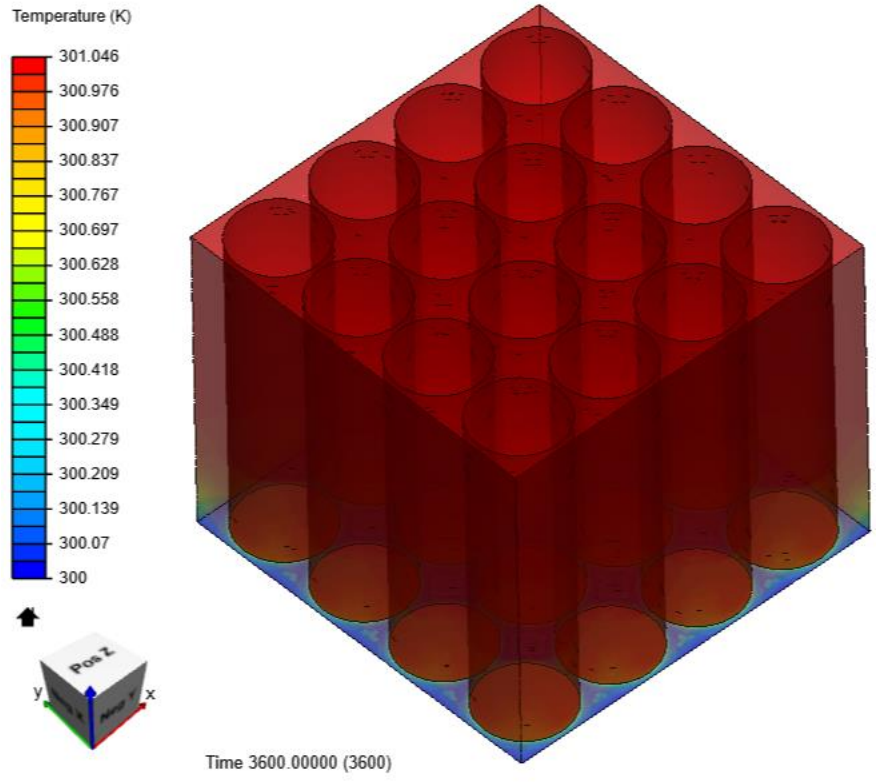

Figure 6.14 : Water with 0.05 m/s velocity and 1C discharge rate

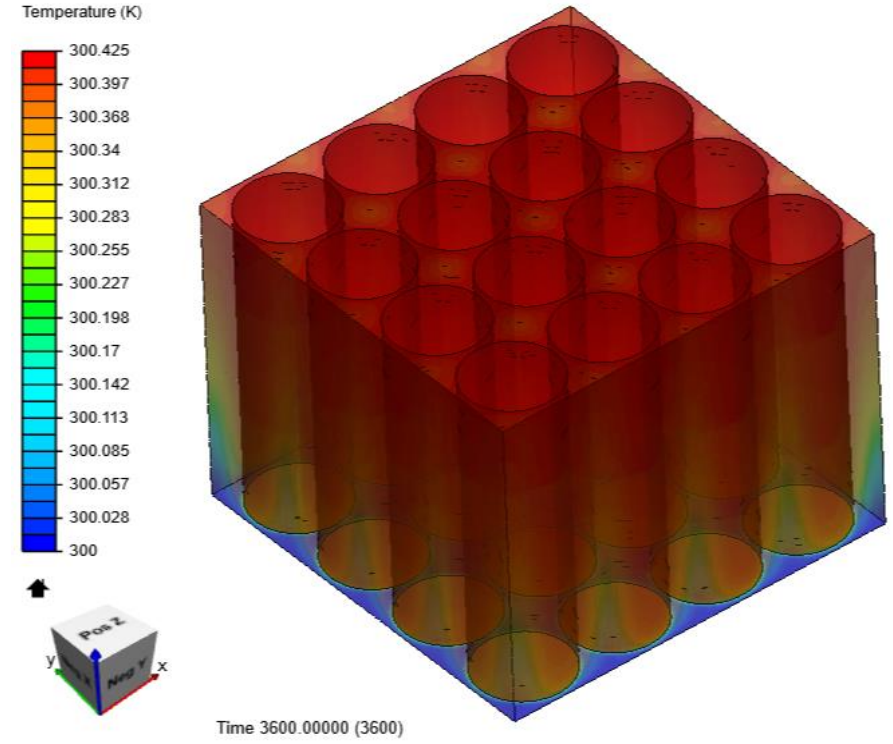

Figure 6.15 : Water with 0.5 m/s velocity and 1C discharge rate

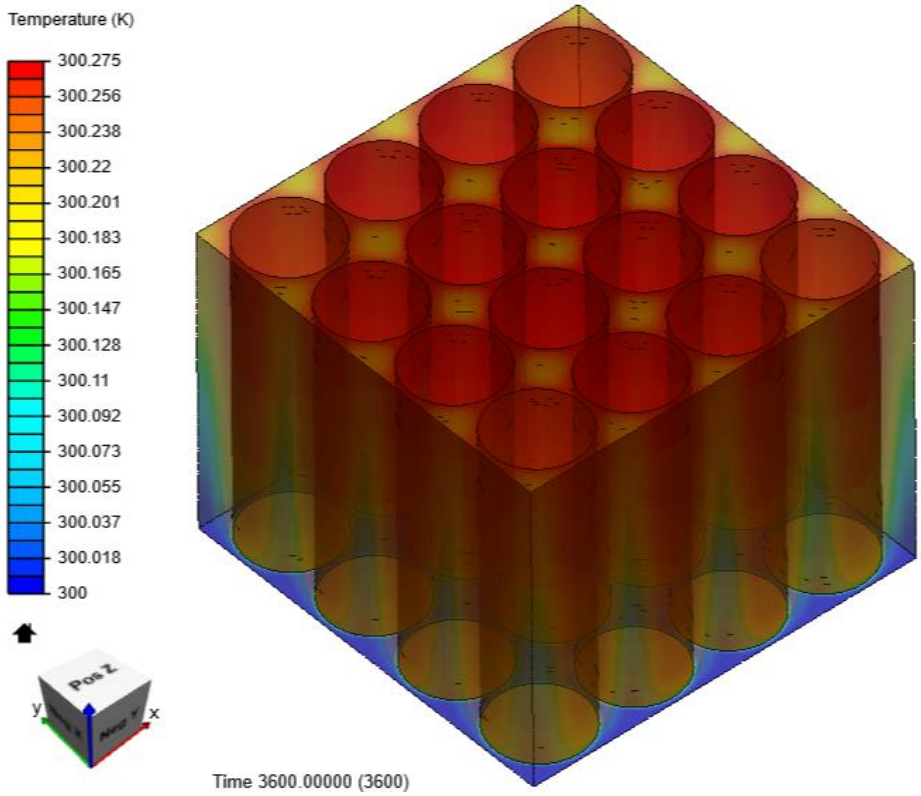

Figure 6.16 : Water with 1 m/s velocity and 1C discharge rate

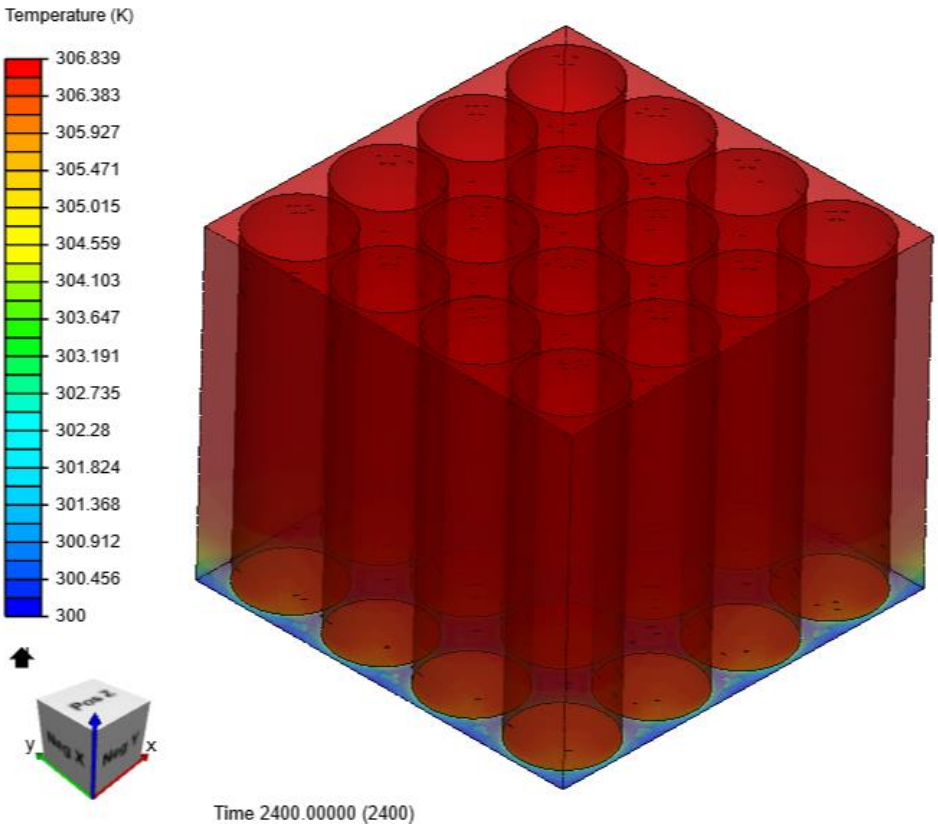

Figure 6.17 : Water with 0.01 m/s velocity and 2C discharge rate

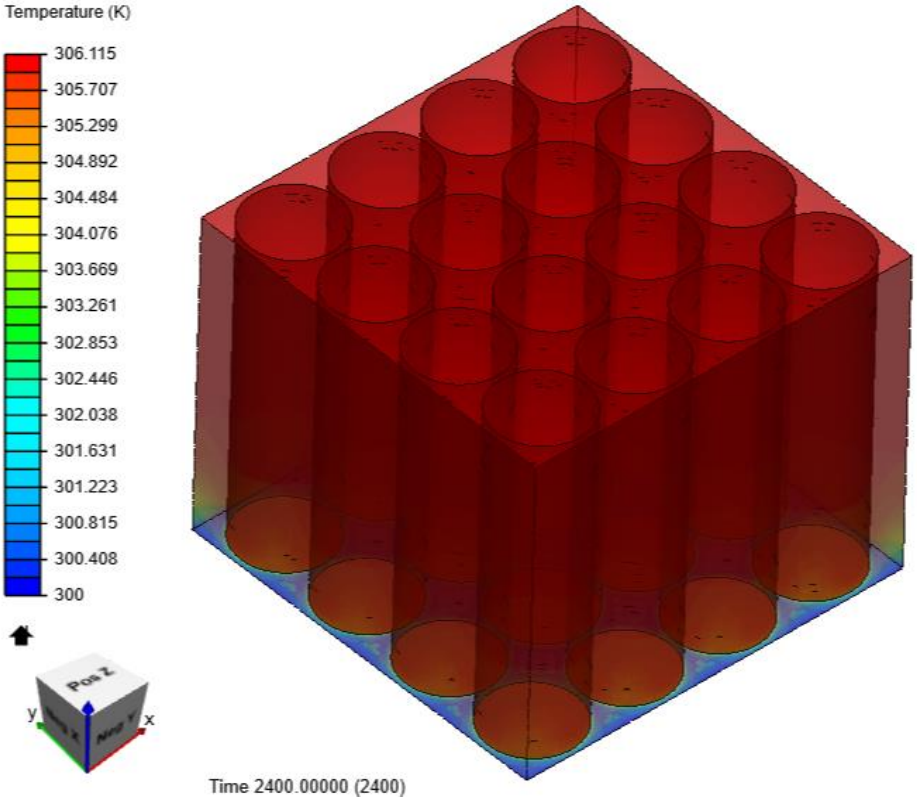

Figure 6.18 : Water with 0.05 m/s velocity and 2C discharge rate

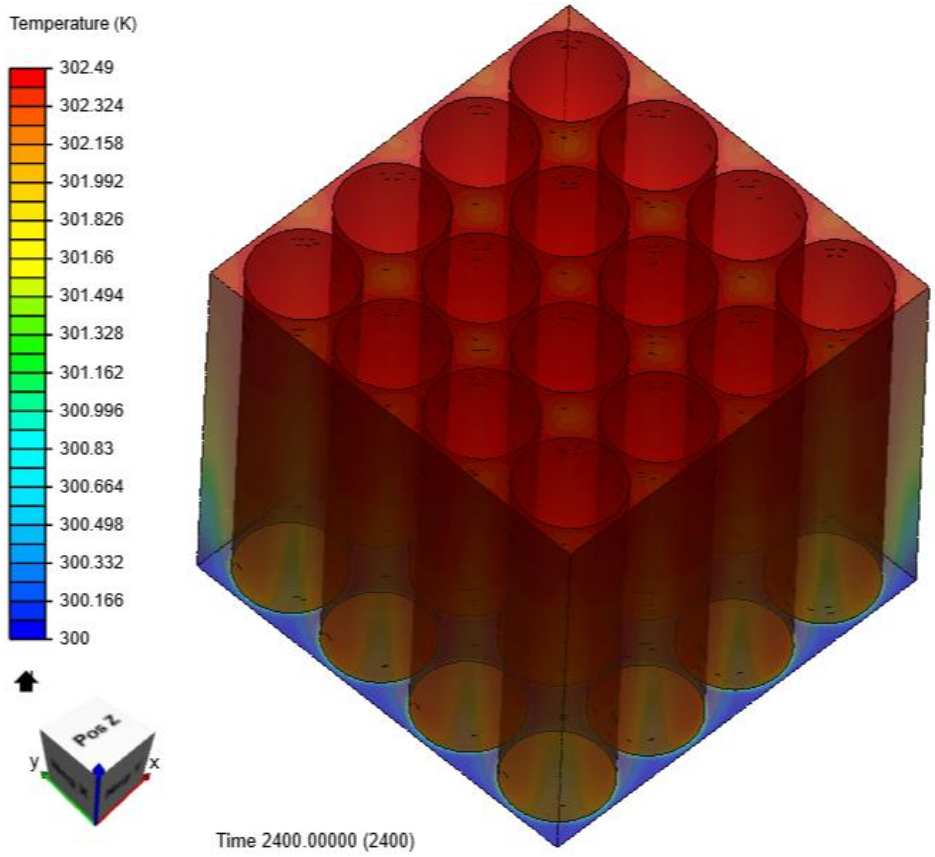

Figure 6.19 : Water with 0.5 m/s velocity and 2C discharge rate

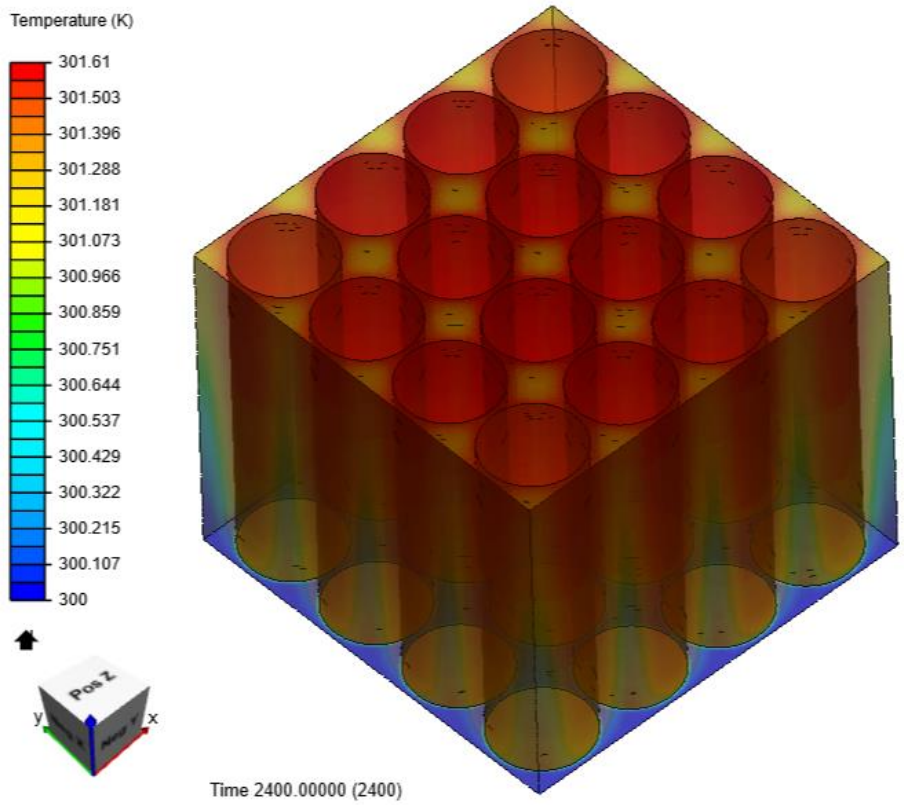

Figure 6.20 : Water with 1 m/s velocity and 2C discharge rate

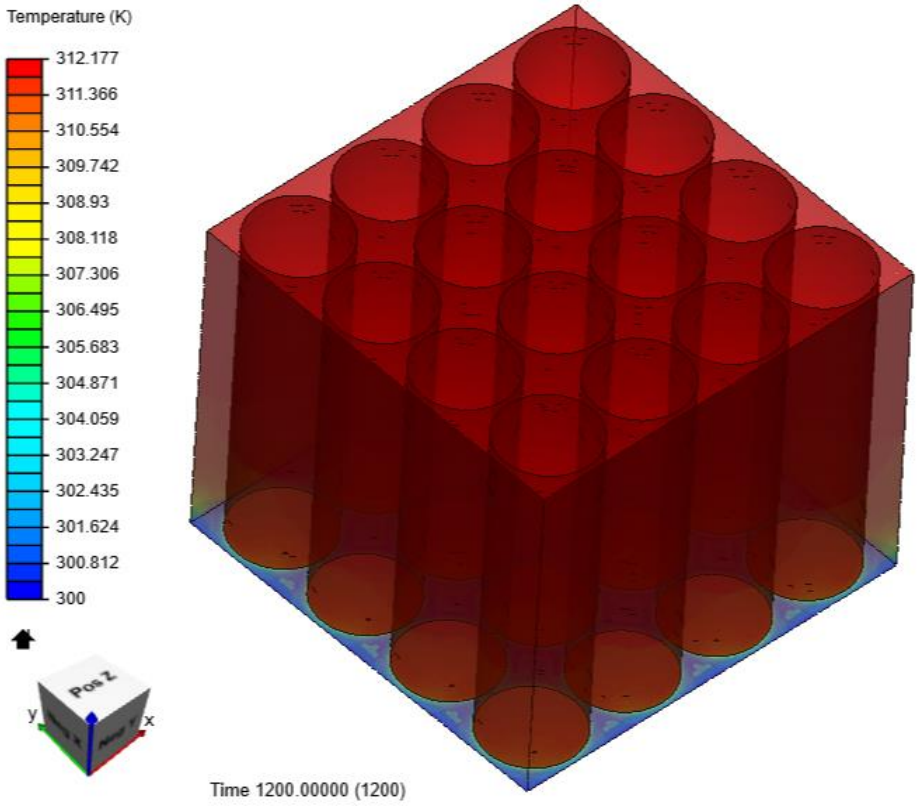

Figure 6.21 : Water with 0.01 m/s velocity and 3C discharge rate

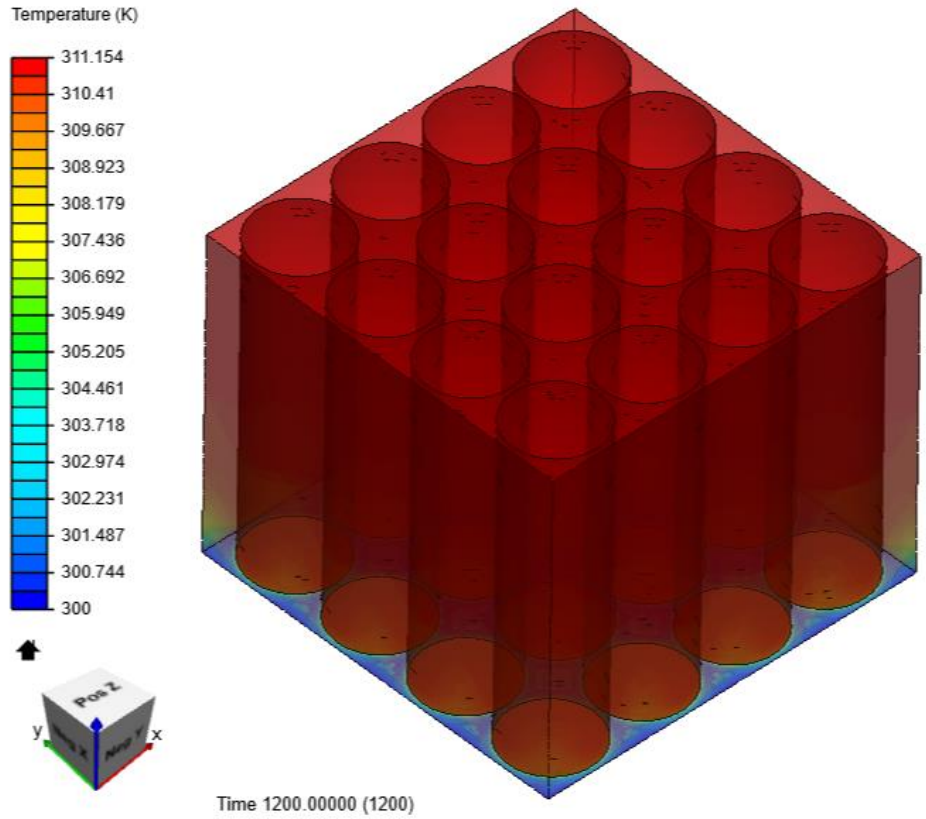

Figure 6.22 : Water with 0.05 m/s velocity and 3C discharge rate

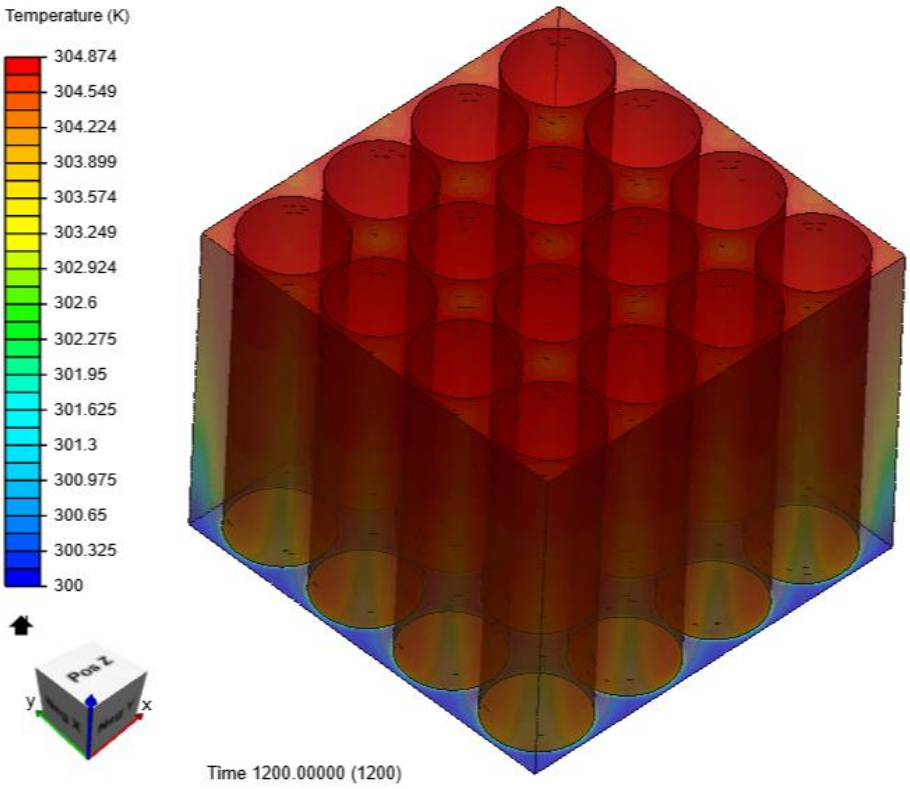

Figure 6.23 : Water with 0.5 m/s velocity and 3C discharge rate

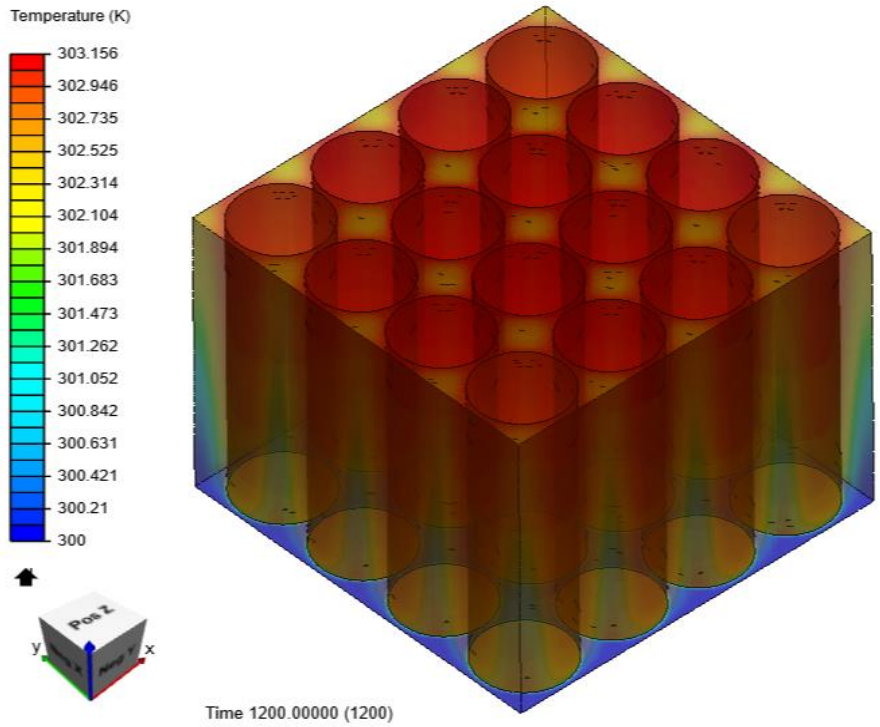

Figure 6.24 : Water with 1 m/s velocity and 3C discharge rate

6.5 DISCUSSION FOR WATER AS COOLANT

CASE	Inlet Velocity (m/s)	Discharge Rate (C)	Maximum Battery Pack Temperature (K)
1	0.01	1C	301.172
2	0.05	1C	301.046
3	0.5	1C	300.425
4	1	1C	300.275
5	0.01	2C	306.839
6	0.05	2C	306.115
7	0.5	2C	302.49
8	1	2C	301.61
9	0.01	3C	312.177
10	0.05	3C	311.154
11	0.5	3C	304.874
12	1	3C	303.156

Table 6.2 : Maximum temperature for various conditions for Water

After air, water is chosen as the cooling fluid and all the 12 cases are simulated. With 1C discharge rate and 0.01m/s inlet velocity the maximum battery pack temperature reaches around 301K.The low discharge rate and higher heat carrying capacity of water is able to limit the temperature from going into the thermal runaway region.

Further increase in the inlet velocity of water doesn't cause much variation in temperature as the discharge rate of 1C produce less heat in the battery pack for which the low velocity water is sufficient to cool the battery.

The discharge rate is varied to 2C which leads to an increment in heat generation hence an increase in maximum battery pack temperature to round about 306K for 0.01m/s and 0.05m/s inlet velocities of water. Higher specific heat capacity and better contact with cell surface is the reason for better cooling effect of water.

With higher inlet velocities of water (0.5m/s and 1m/s) the battery pack temperature reduces by 4K and 5K respectively.

The discharge rate of the cells is increased to 3C causing further increment in heat generation and increment in battery temperature to 312K and 311K for 0.01m/s and 0.05m/s inlet velocity of water respectively. These temperatures are in the upper half of the optimum range hence the cooling could be improved by increasing the

inlet velocity of water to 0.5m/s resulting in lowering of the battery temperature to about 305K which is within the optimum range. Further increment in the inlet velocity to 1m/s brings down the maximum battery pack temperature to 303K.

6.6 RESULTS WITH WATER-ETHYLENE GLYCOL(7%) AS COOLANT

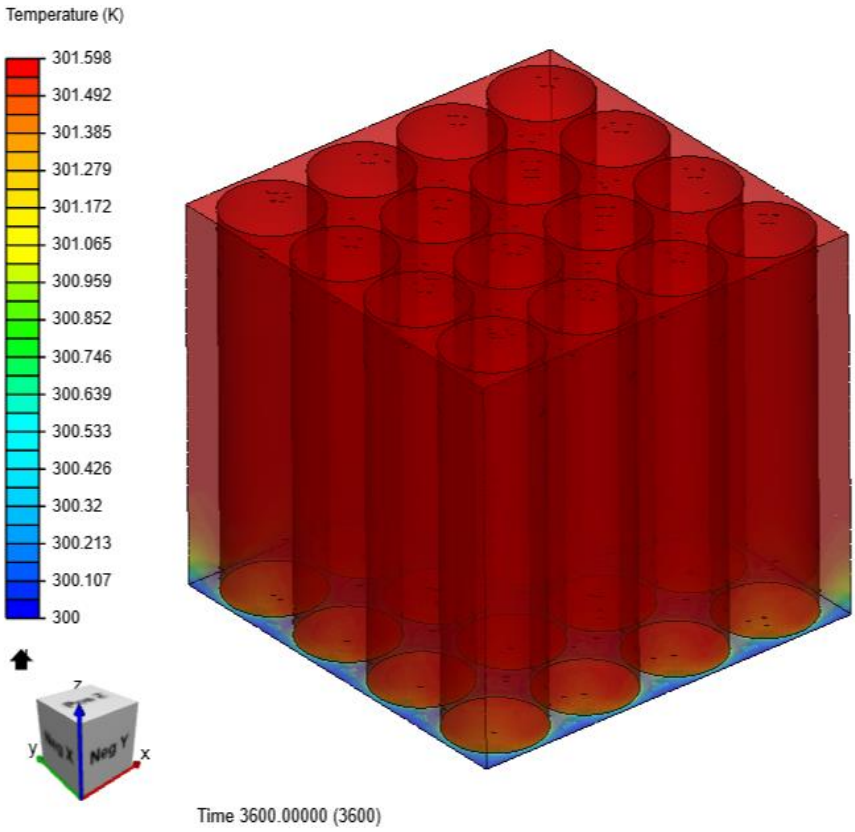

Figure 6.25 : Water-Ethylene glycol (7%) with 0.01 m/s velocity and 1C discharge rate

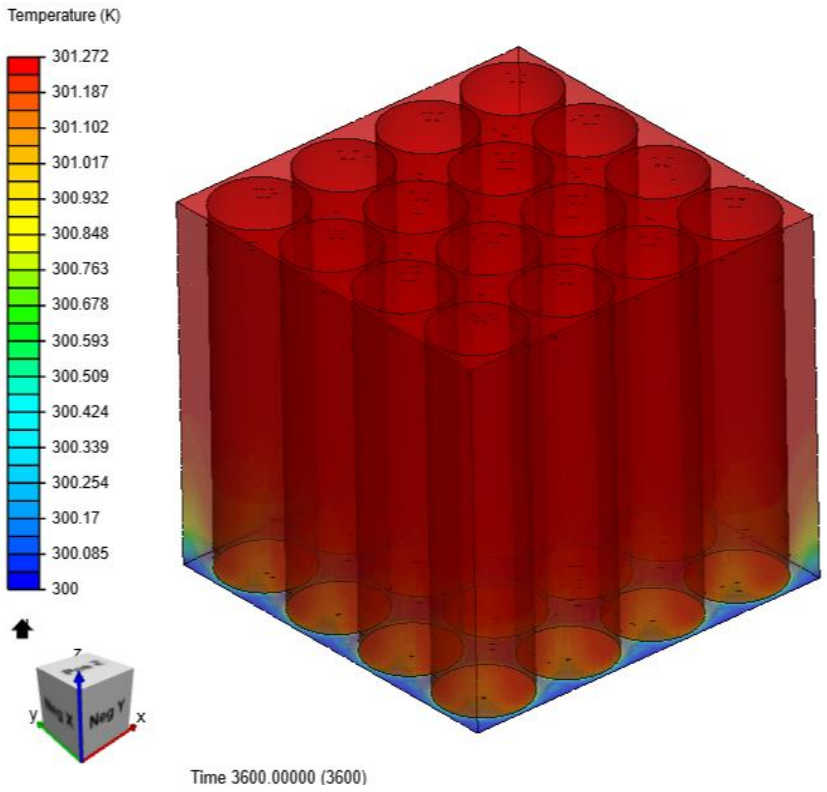

Figure 6.26 : Water-Ethylene glycol (7%) with 0.05 m/s velocity and 1C discharge rate

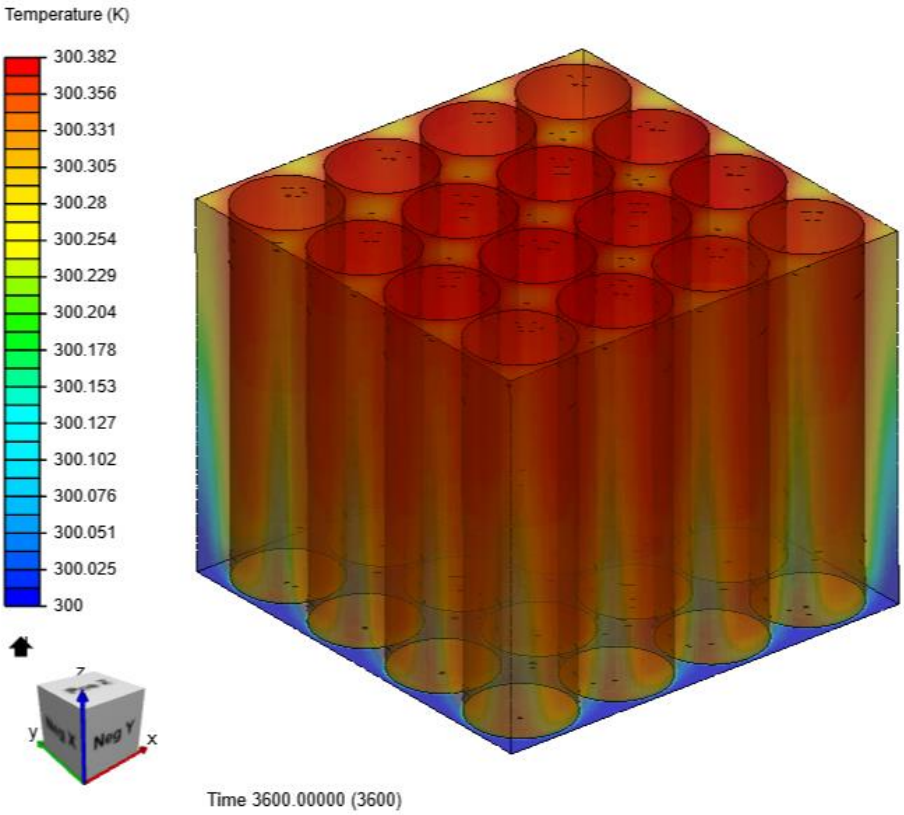

Figure 6.27 : Water-Ethylene glycol (7%) with 0.5 m/s velocity and 1C discharge rate

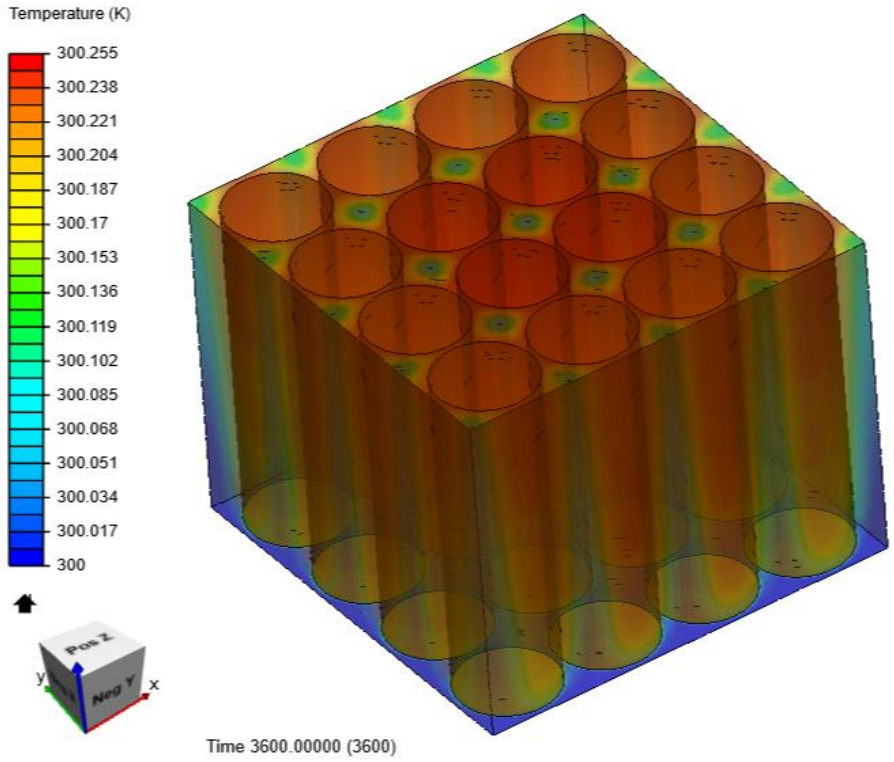

Figure 6.28 : Water-Ethylene glycol (7%) with 1 m/s velocity and 1C discharge rate

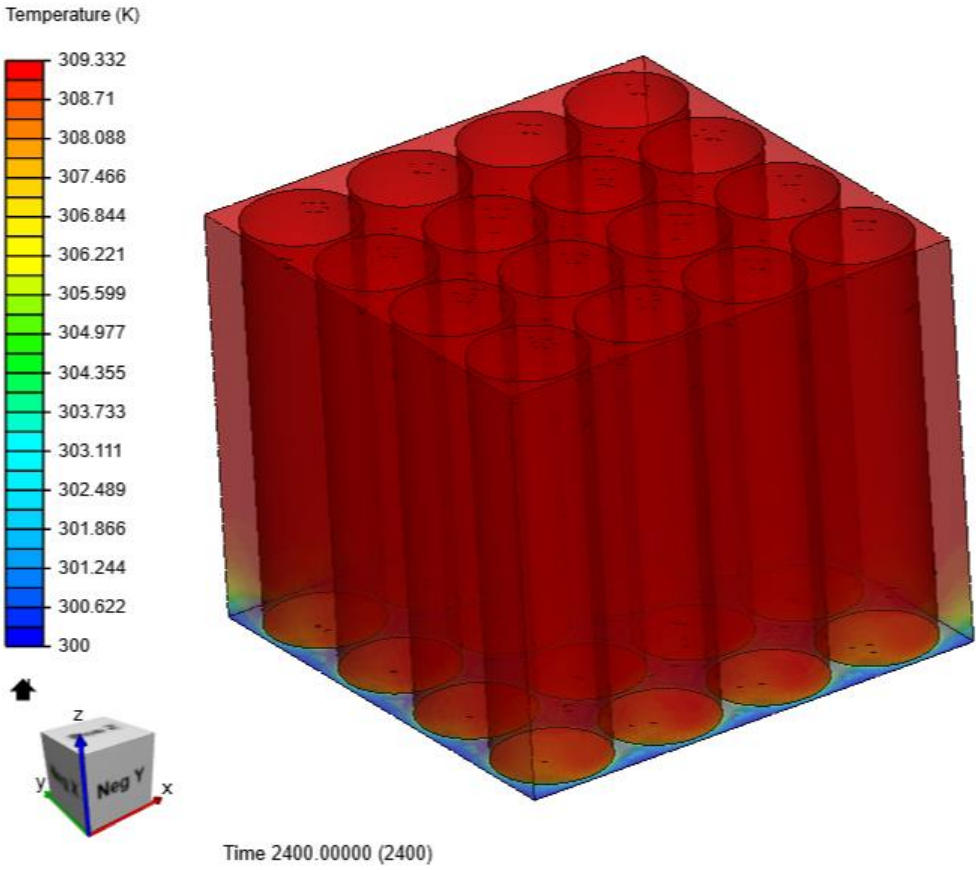

Figure 6.29 : Water-Ethylene glycol (7%) with 0.01 m/s velocity and 2C discharge rate

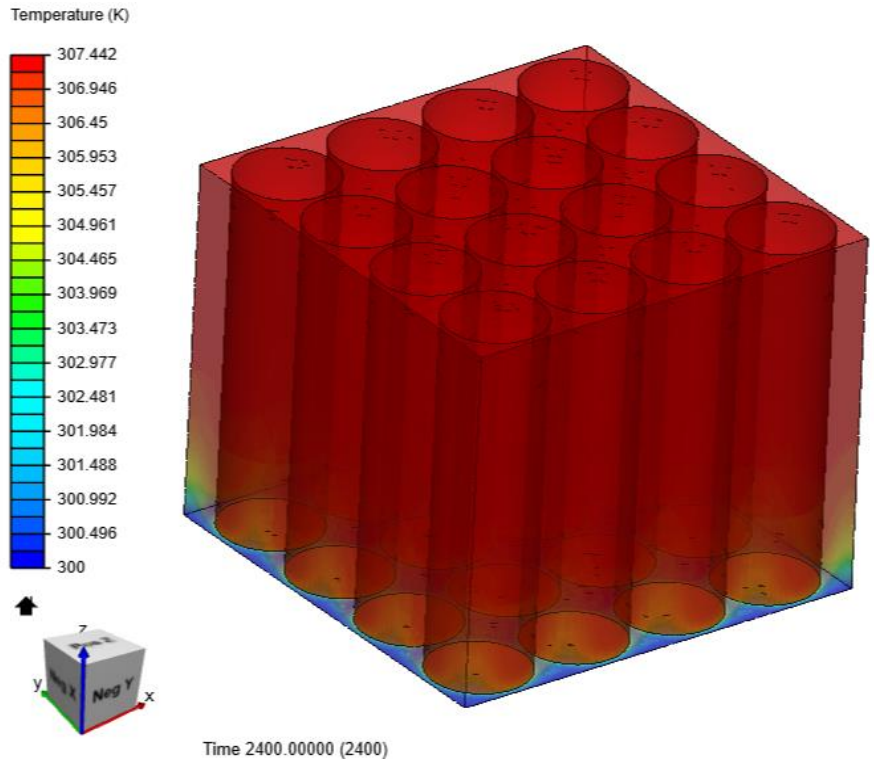

Figure 6.30 : Water-Ethylene glycol (7%) with 0.05 m/s velocity and 2C discharge rate

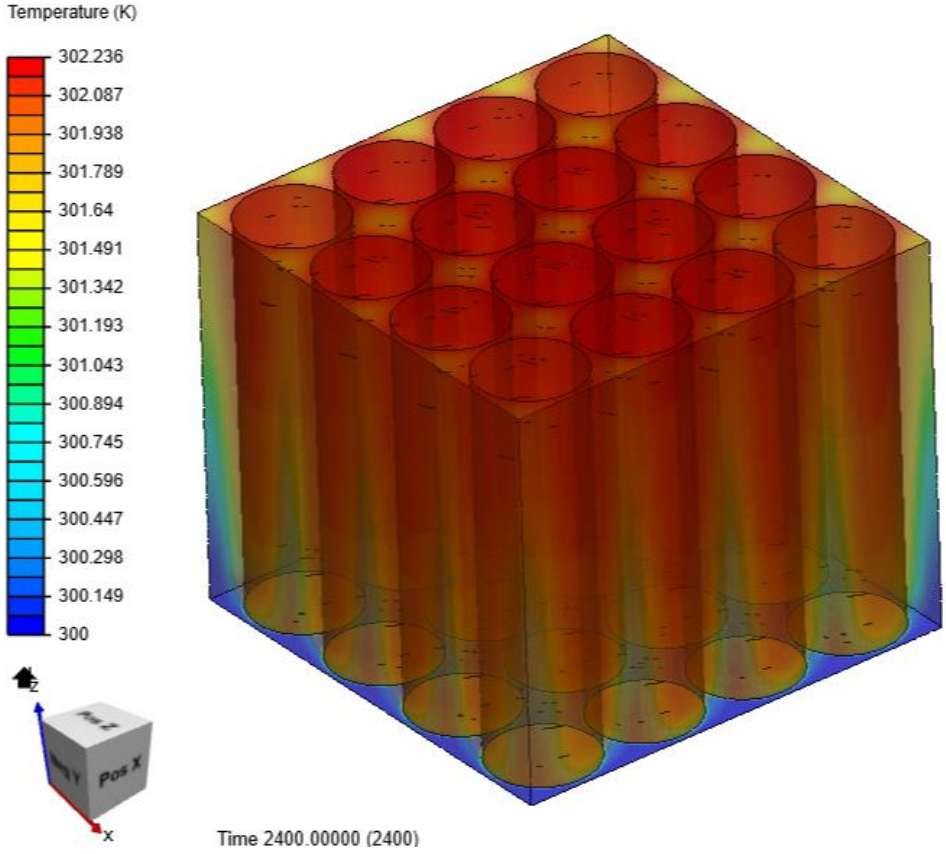

Figure 6.31 : Water-Ethylene glycol (7%) with 0.5 m/s velocity and 2C discharge rate

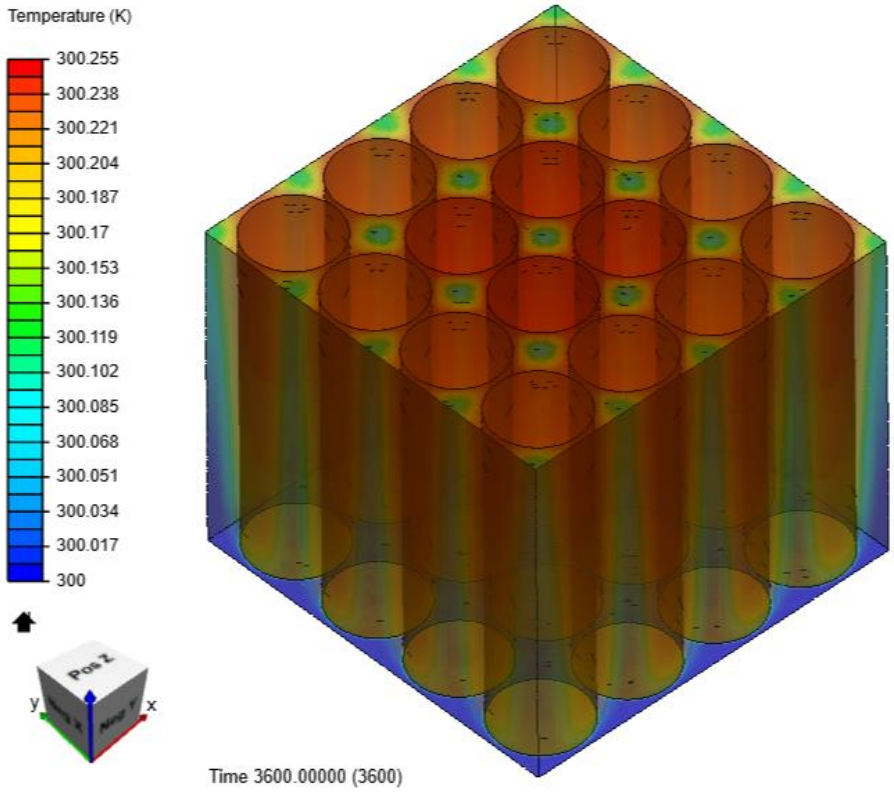

Figure 6.32 : Water-Ethylene glycol (7%) with 1 m/s velocity and 2C discharge rate

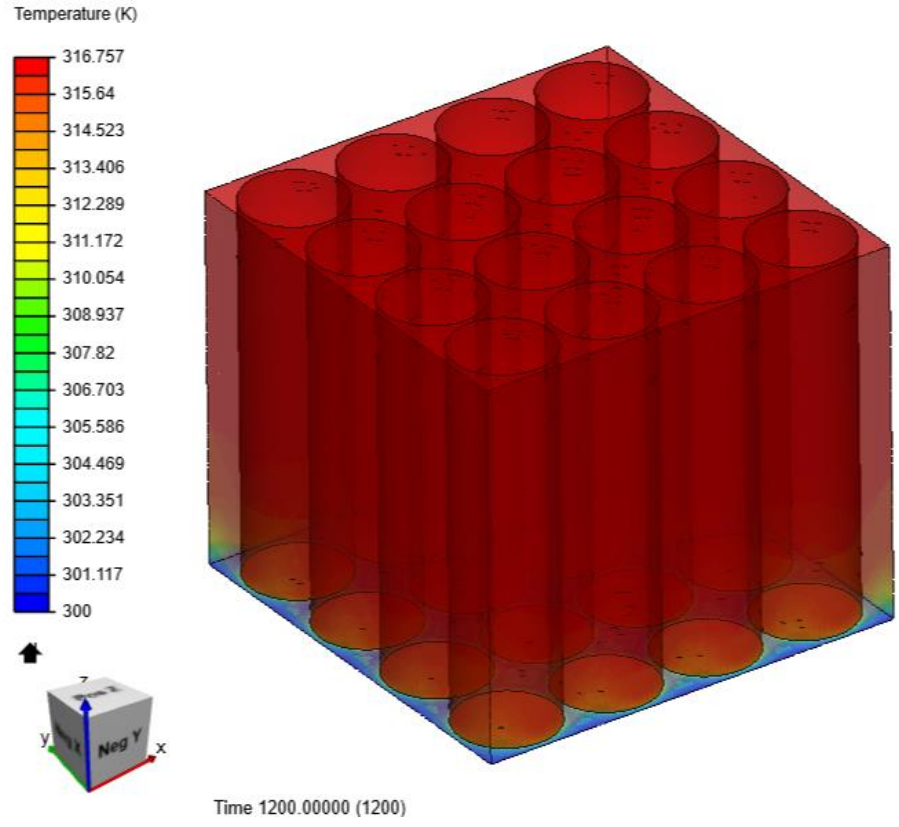

Figure 6.33 : Water-Ethylene glycol (7%) with 0.01 m/s velocity and 3C discharge rate

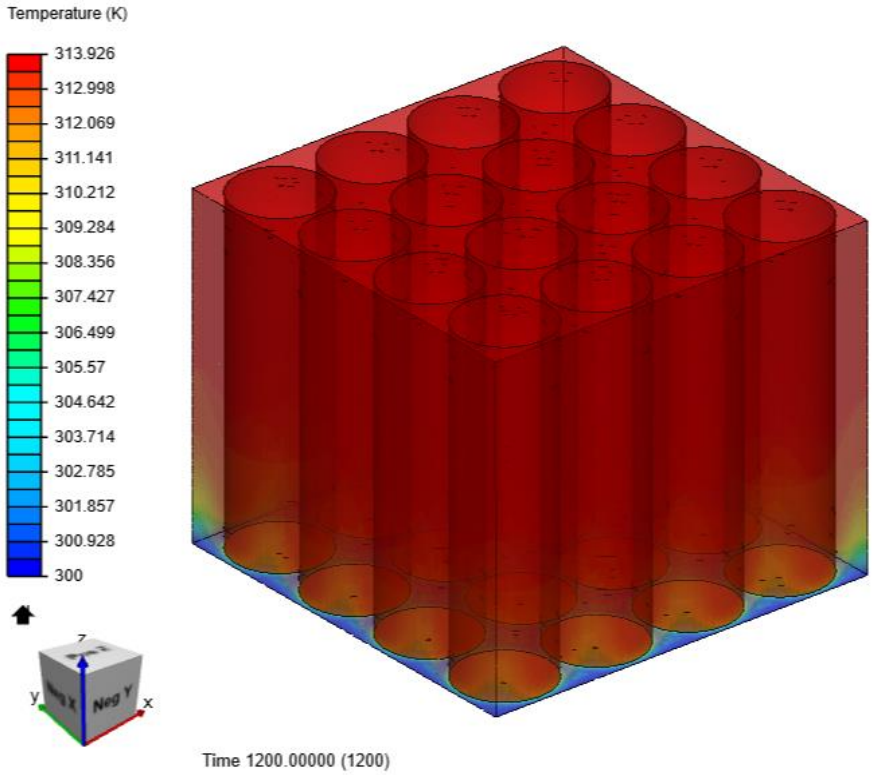

Figure 6.34 : Water-Ethylene glycol (7%) with 0.05 m/s velocity and 3C discharge rate

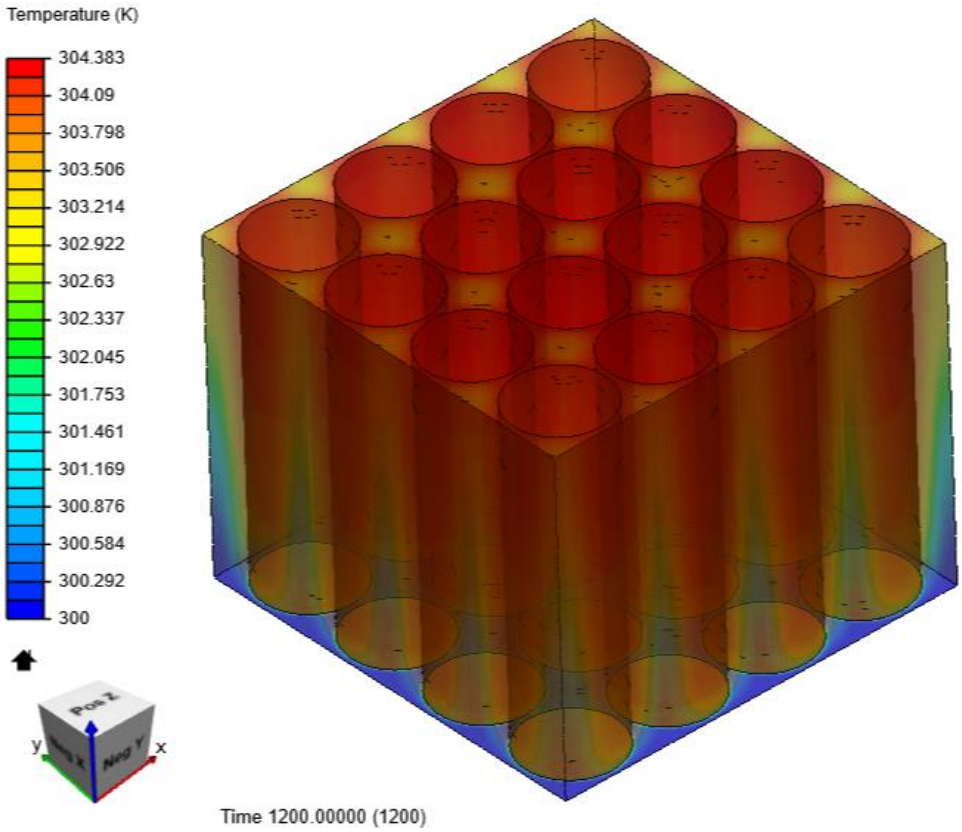

Figure 6.35 : Water-Ethylene glycol (7%) with 0.5 m/s velocity and 3C discharge rate

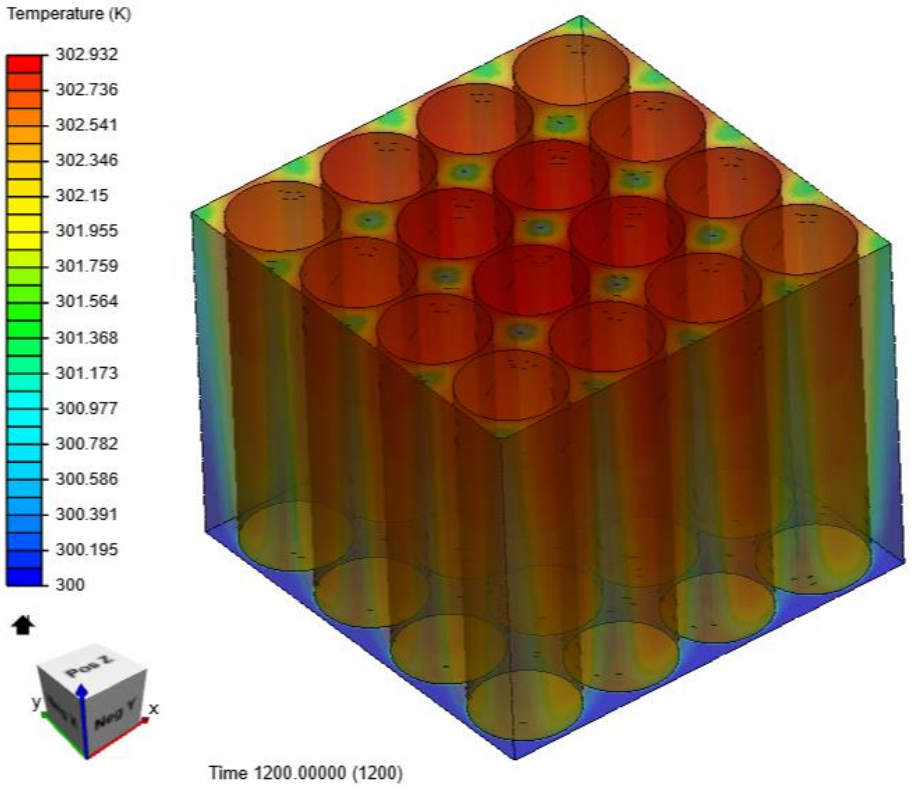

Figure 6.36 : Water-Ethylene glycol (7%) with 1 m/s velocity and 3C discharge rate

6.7 DISCUSSION FOR WATER–ETHYLENE GLYCOL (7%) AS COOLANT

CASE	Inlet Velocity (m/s)	Discharge Rate (C)	Maximum Battery Pack Temperature (K)
1	0.01	1C	301.598
2	0.05	1C	301.272
3	0.5	1C	300.382
4	1	1C	300.255
5	0.01	2C	309.332
6	0.05	2C	307.442
7	0.5	2C	302.236
8	1	2C	301.496
9	0.01	3C	316.757
10	0.05	3C	313.926
11	0.5	3C	304.383
12	1	3C	302.932

Table 6.3 : Maximum temperature for various conditions for **Water + Ethylene Glycol (7%)**

After water,7% of ethylene glycol is mixed with water and is selected as the cooling fluid and all the 12 cases are simulated. With 1C discharge rate and 0.01m/s inlet velocity the maximum battery pack temperature reaches around 301K.The low discharge rate and higher heat carrying capacity of the mixture is able to limit the temperature from going into the thermal runaway region.

Further increase in the inlet velocity of water doesn't cause much variation in temperature as the discharge rate of 1C produce less heat in the battery pack for which the low velocity water-ethylene glycol mixture is sufficient to cool the battery.

The discharge rate is varied to 2C which leads to an increment in heat generation hence an increase in maximum battery pack temperature to round about 309K and 307K for 0.01m/s and 0.05m/s inlet velocities of the water-ethylene glycol mixture respectively. Higher specific heat capacity and better contact with cell surface is the reason for better cooling effect of water.

With higher inlet velocities of air (0.5m/s and 1m/s) the battery pack temperature reduces by 5K and 6K respectively.

The discharge rate of the cells is increased to 3C causing further increment in heat generation and increment in battery temperature to 317K and 314K for 0.01m/s and 0.05m/s inlet velocity of water-ethylene glycol mixture respectively. These temperatures are in the upper half of the optimum range hence the cooling could be improved by increasing the inlet velocity of water-ethylene glycol mixture to 0.5m/s resulting in lowering of the battery temperature to about 304K which is within the optimum range. Further increment in the inlet velocity to 1m/s brings down the maximum battery pack temperature to 303K. The presence of ethylene glycol increases the antifreeze property of the coolant and also lowers the specific heat slightly.

6.8 RESULTS WITH WATER-1% Al_2O_3 AS COOLANT

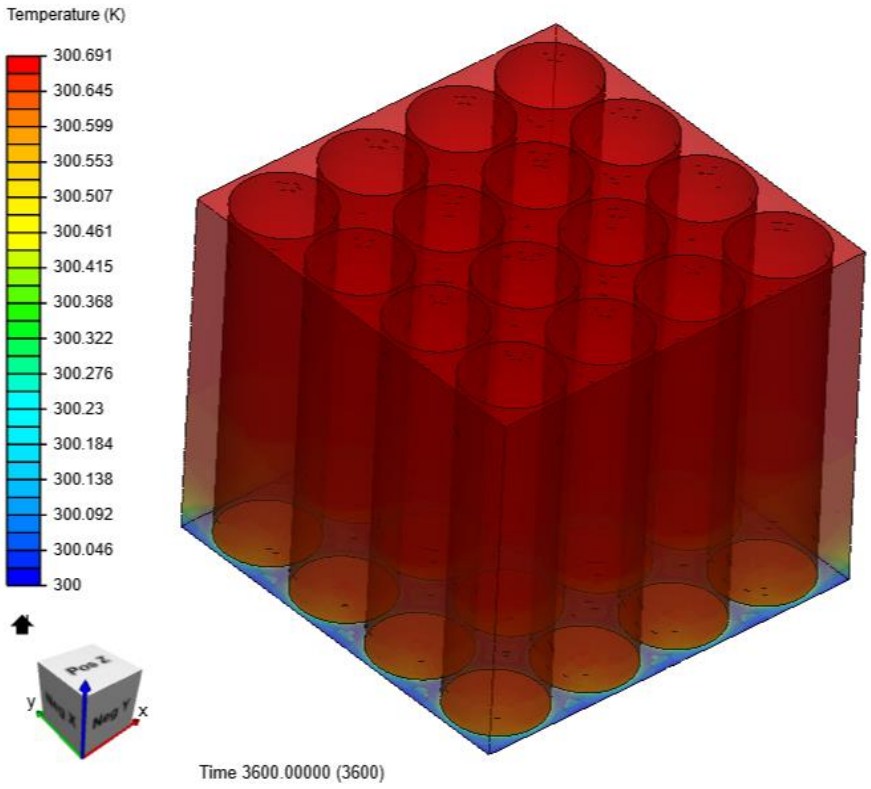

Figure 6.37 : Water - 1% Al_2O_3 with 0.01 m/s velocity and 1C discharge rate

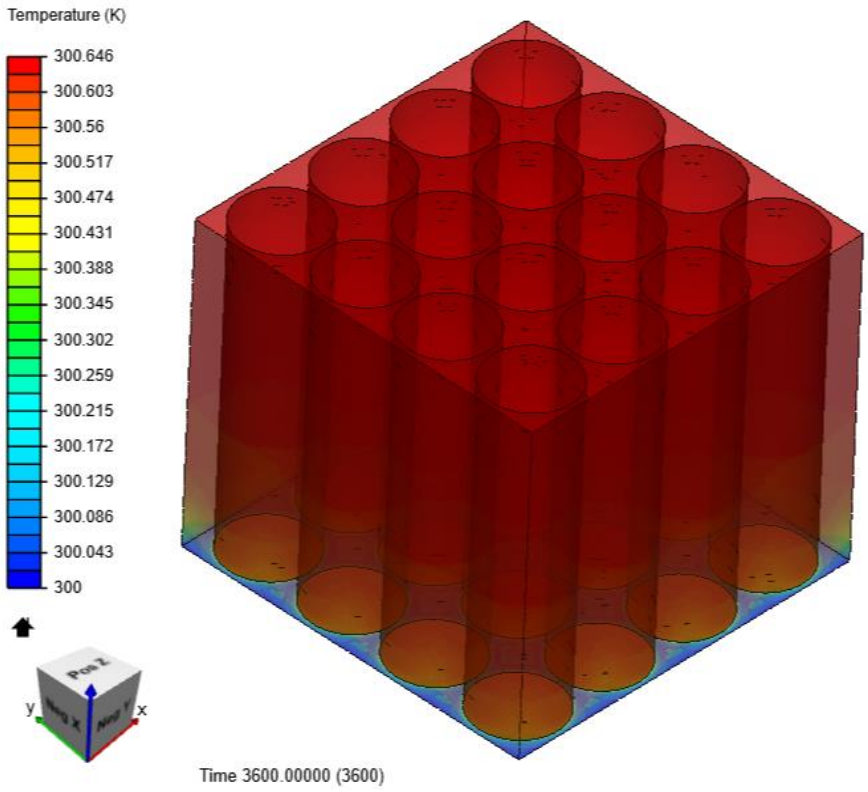

Figure 6.38 : Water - 1% Al_2O_3 with 0.05 m/s velocity and 1C discharge rate

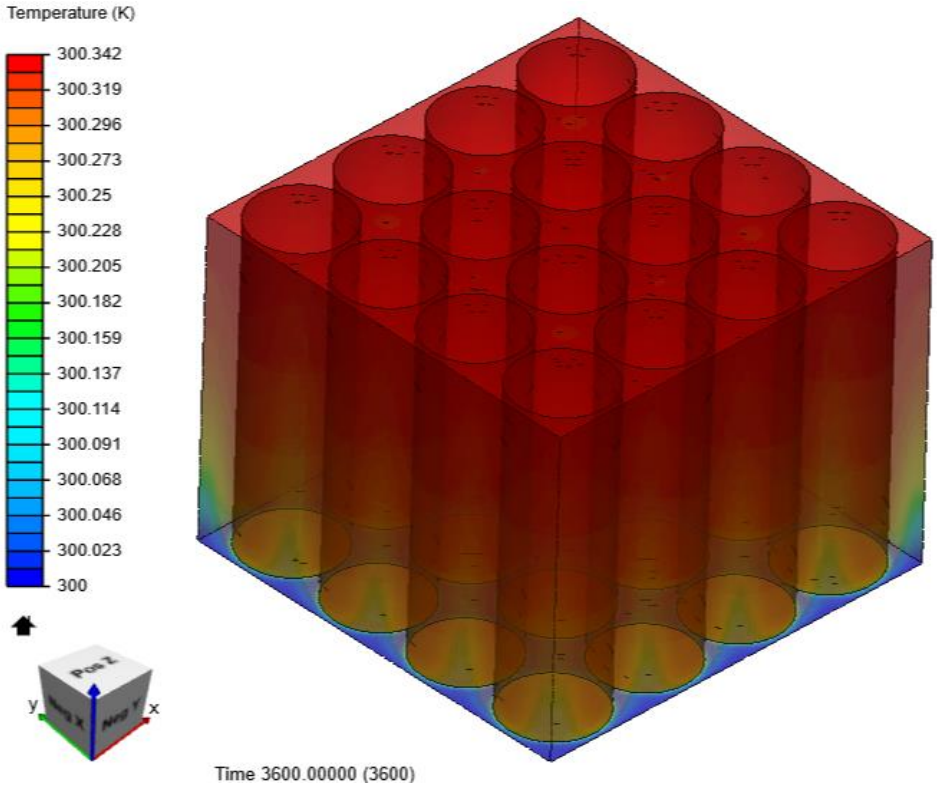

Figure 6.39 : Water - 1% Al_2O_3 with 0.5 m/s velocity and 1C discharge rate

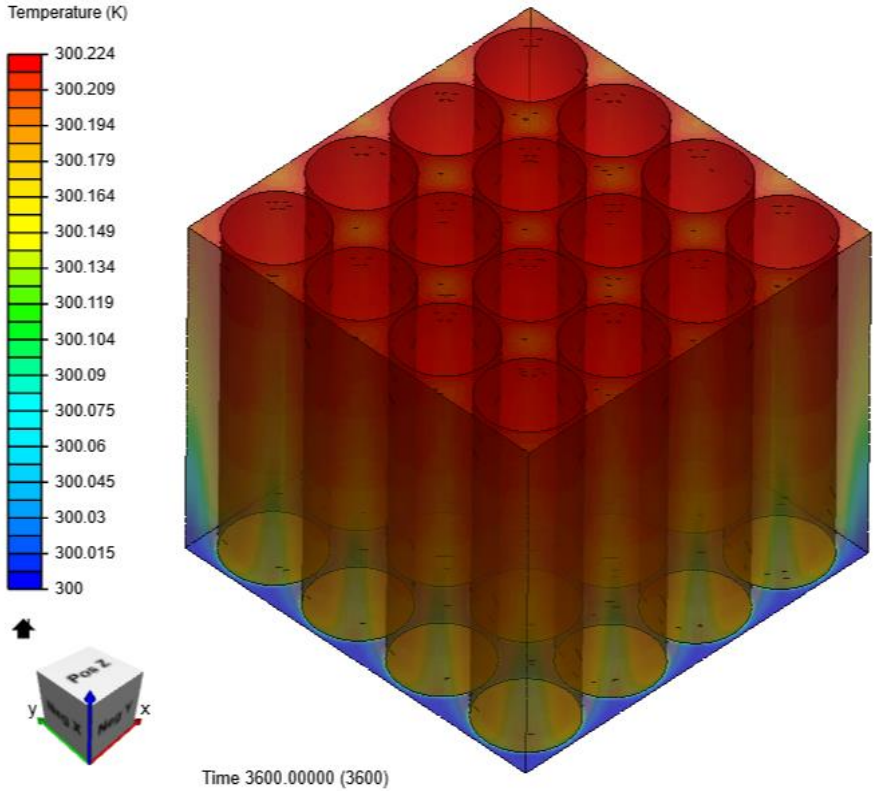

Figure 6.40 : Water - 1% Al_2O_3 with 1 m/s velocity and 1C discharge rate

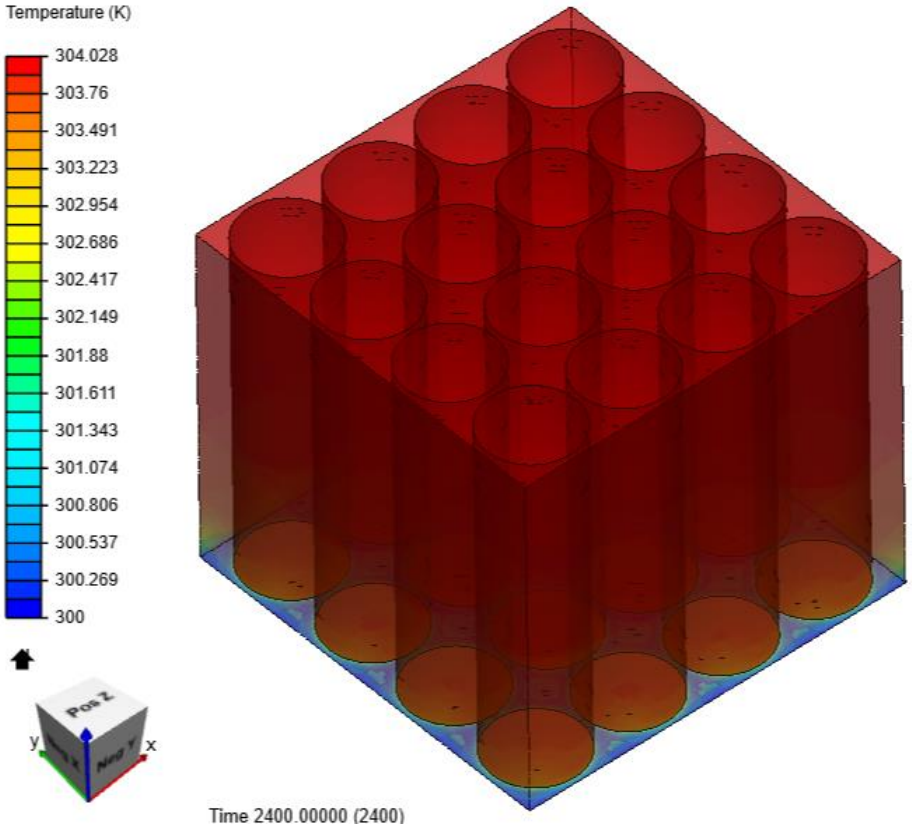

Figure 6.41 : Water - 1% Al_2O_3 with 0.01 m/s velocity and 2C discharge rate

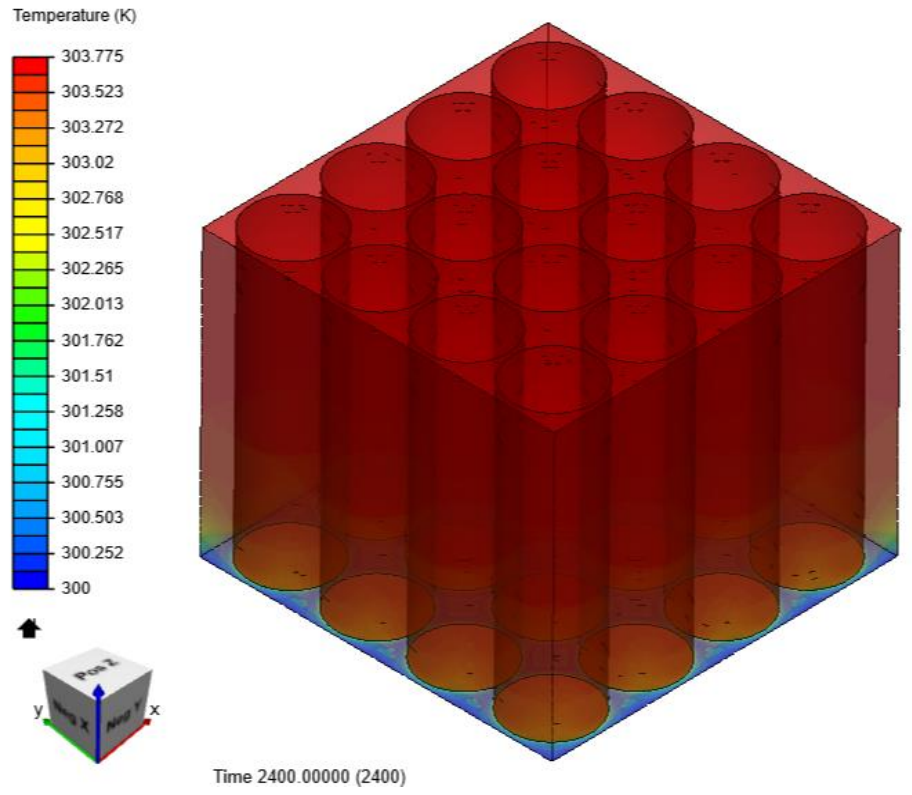

Figure 6.42 : Water - 1% Al_2O_3 with 0.05 m/s velocity and 2C discharge rate

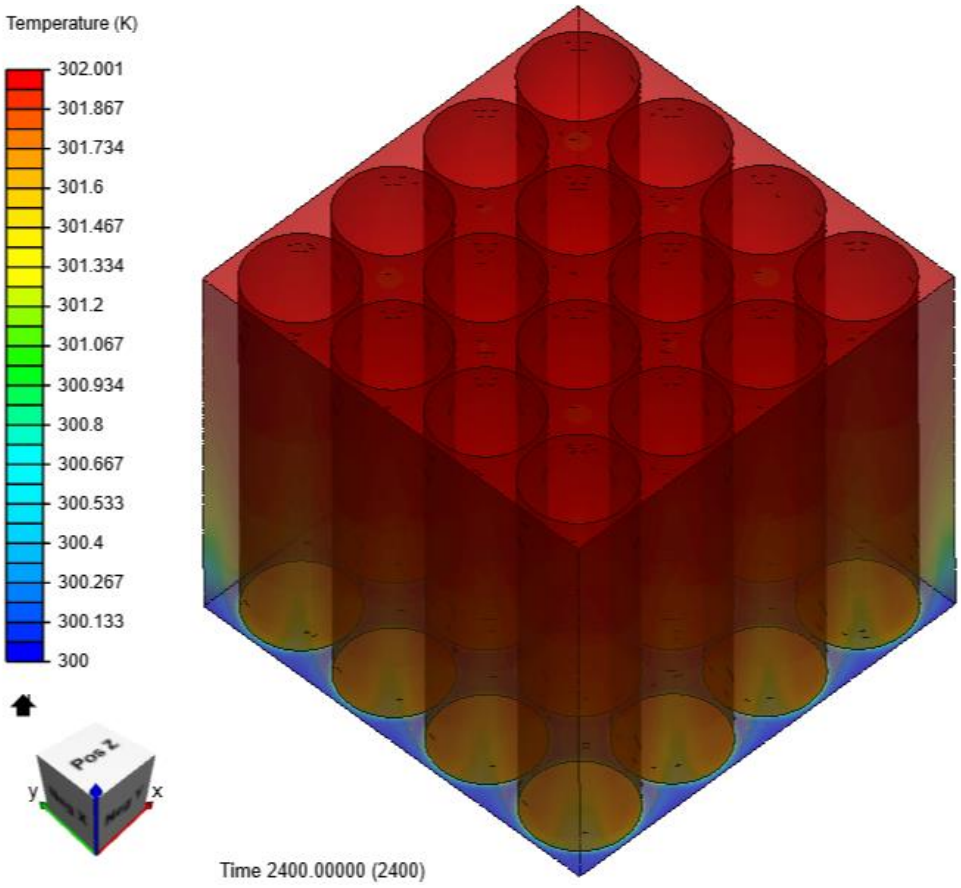

Figure 6.43 : Water - 1% Al_2O_3 with 0.5 m/s velocity and 2C discharge rate

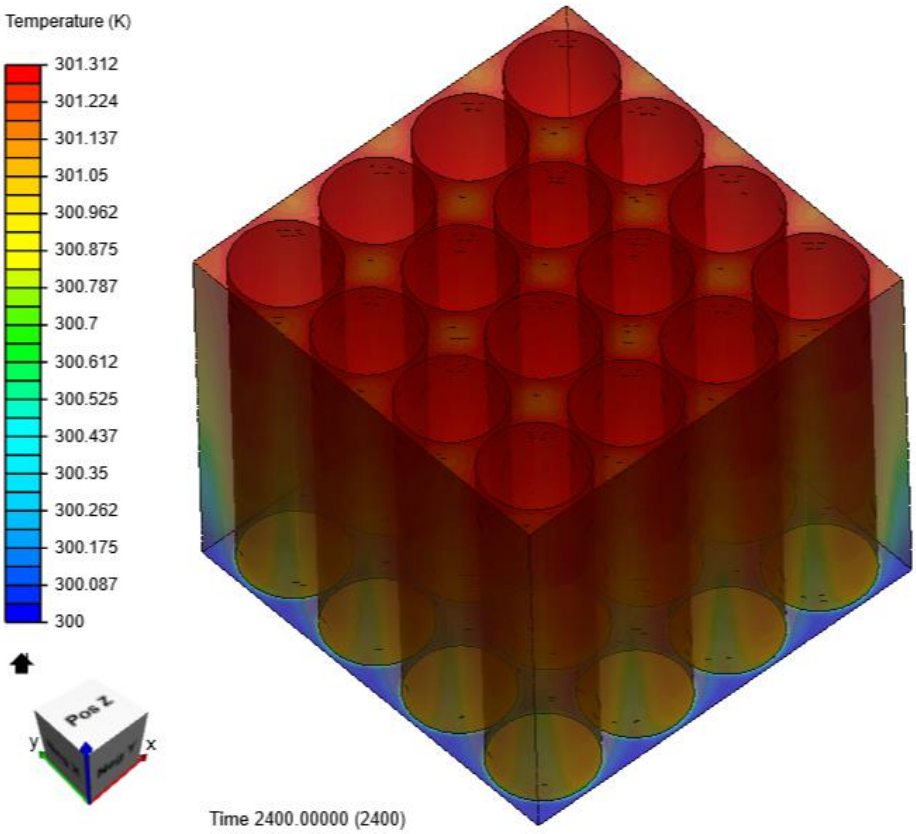

Figure 6.44 : Water - 1% Al_2O_3 with 1 m/s velocity and 2C discharge rate

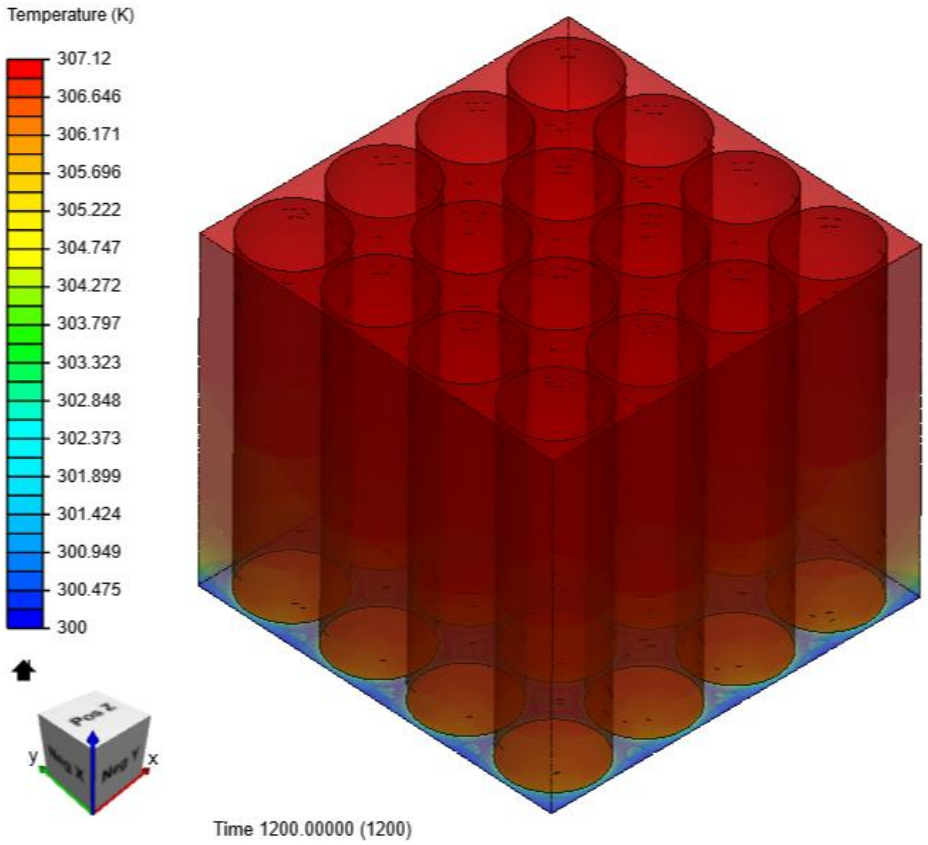

Figure 6.45 : Water - 1% Al_2O_3 with 0.01 m/s velocity and 3C discharge rate

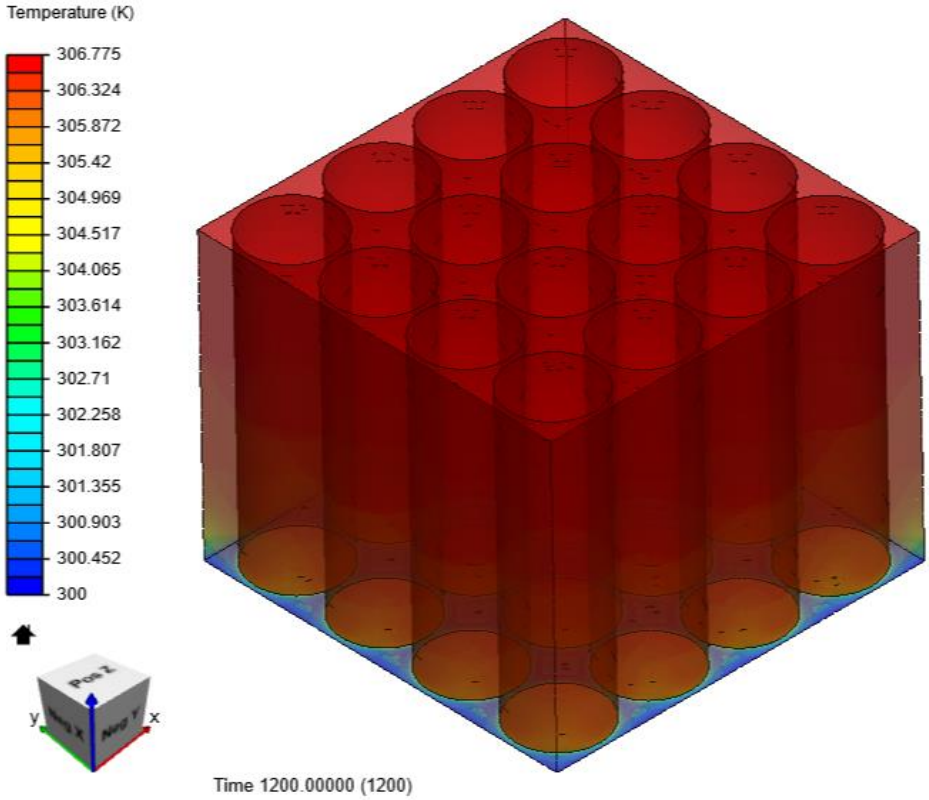

Figure 6.46 : Water - 1% Al_2O_3 with 0.05 m/s velocity and 3C discharge rate

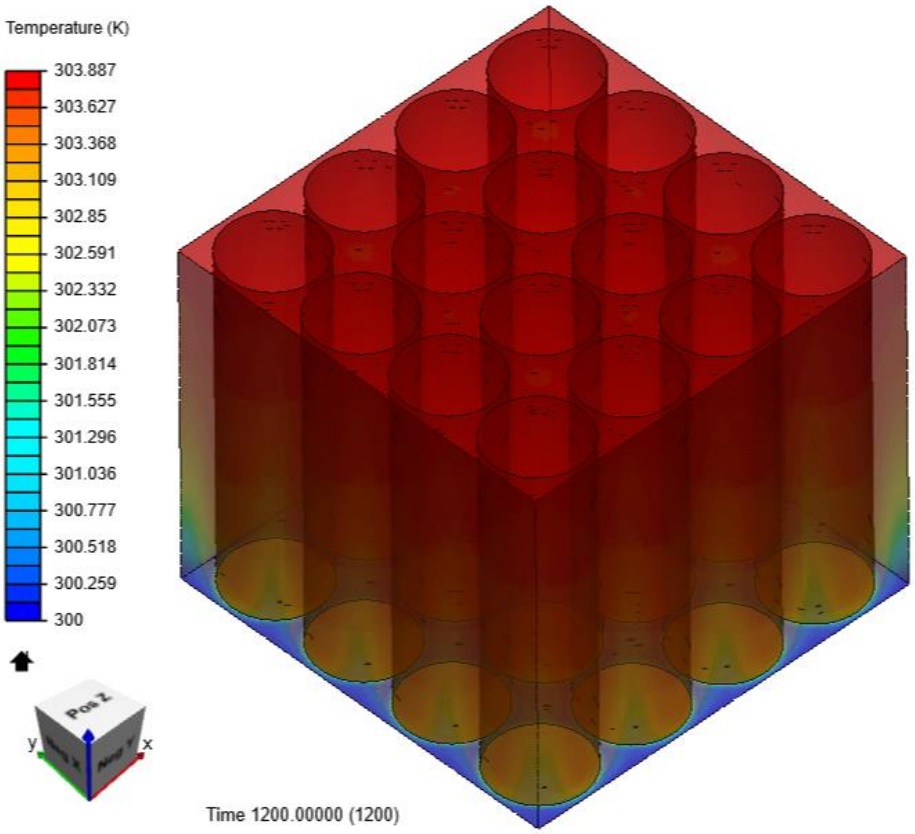

Figure 6.47 : Water - 1% Al_2O_3 with 0.5 m/s velocity and 3C discharge rate

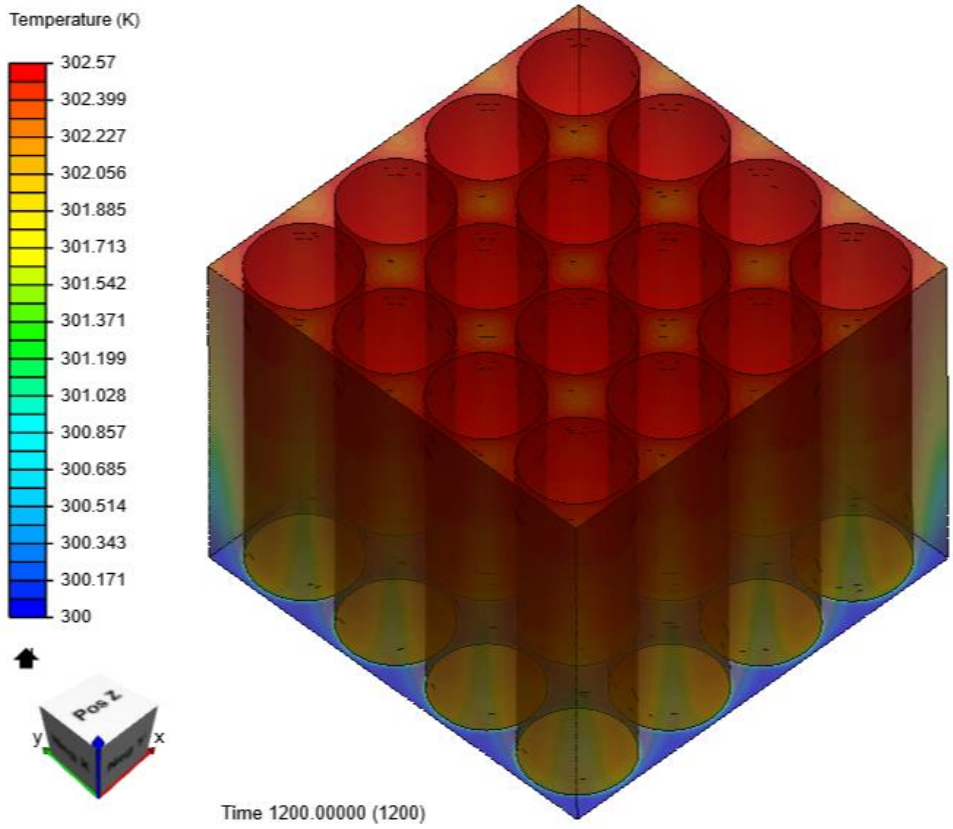

Figure 6.48 : Water - 1% Al_2O_3 with 1 m/s velocity and 3C discharge rate

6.9 DISCUSSION FOR WATER - Al_2O_3 AS COOLANT

CASE	Inlet Velocity (m/s)	Discharge Rate (C)	Maximum Battery Pack Temperature (K)
1	0.01	1C	300.691
2	0.05	1C	300.646
3	0.5	1C	300.342
4	1	1C	300.224
5	0.01	2C	304.028
6	0.05	2C	303.775
7	0.5	2C	302.001
8	1	2C	301.312
9	0.01	3C	307.12
10	0.05	3C	306.775
11	0.5	3C	303.887
12	1	3C	302.57

Table 6.4 : Maximum temperature for various conditions for **Water + 1% Al_2O_3**

Finally, 1% of aluminium oxide is used along with water to form nanofluid mixture and is selected as the cooling fluid and all the 12 cases are simulated. With 1C discharge rate and 0.01m/s inlet velocity the maximum battery pack temperature reaches around 300.7K. The low discharge rate, higher surface area for heat transfer and higher heat carrying capacity of the mixture is able to limit the temperature from going into the thermal runaway region.

Further increase in the inlet velocity of water doesn't cause much variation in temperature as the discharge rate of 1C produce less heat in the battery pack for which the low velocity water-aluminium oxide nanofluid mixture is sufficient to cool the battery.

The discharge rate is varied to 2C which leads to an increment in heat generation hence an increase in maximum battery pack temperature to round about 304K for 0.01m/s and 0.05m/s inlet velocities of the water-ethylene glycol mixture respectively. Higher specific heat capacity and larger surface area for heat transfer are the reason for better cooling effect of water-aluminium oxide nanofluid.

With higher inlet velocities of air (0.5m/s and 1m/s) the battery pack temperature reduces by about 2K and 3K respectively.

The discharge rate of the cells is increased to 3C causing further increment in heat generation and increment in battery temperature to about 307K for 0.01m/s and 0.05m/s inlet velocity of water-aluminium oxide nanofluid respectively. This temperature is within the safe working range. Increasing the inlet velocity of water to 0.5m/s results in lowering of the battery temperature to about 304K which is within the optimum range. Further increment in the inlet velocity to 1m/s brings down the maximum battery pack temperature to 302.5K. The presence of 1% aluminium oxide particles increases the area available for heat transfer (higher thermal conductivity) thereby making the water-aluminium oxide nanofluid mixture a better coolant.

Chapter 7

Conclusion and Scope for Future Work

CHAPTER 7

CONCLUSION AND SCOPE FOR FUTURE WORK

7.1 CONCLUSION

In this research, we have conducted the simulation of cooling of multicell Li-ion 18650 battery. The battery model was created in CATIA v5. The model was simulated in SimScale using Conjugate Heat Transfer Model.

The mathematical modelling made us to understand the internal working of cell and mechanism of heat transfer due to conjugat heat transfer. The analytical method used has computational limitation.The developed method of analysis for cooling gives satisfactory results for thermal management. Among the fluids considered, Al_2O_3 nanofluids gave better results. The method of cooling employed was able to restrict the temperature within the safe operating temperature range. Cooling with air was insufficient for higher discharge rates. The difference between the effect of water and water-ethylene glycol hybrid fluid was mere for smaller discharges and difference was quite noticeable for higher discharge rates. Nanofluids performed better under almost all conditons. This accounts for their higher conductivity and heat capacityAl_2O_3 nanofluid coolant at 0.5m/s was optimum for all cases. The temperature sensitive hotspots were reduced. These results are in good agreement with the proven temperature range required for the efficient running of battery in electric vehicles which are available from the literature.

7.2 SCOPE FOR FUTURE WORK

In an era of depleting oil reserves, the turmoil of the energy crisis is getting worse every year. The conventional sources are failing to meet the need of mankind. Electricity can be produced by numerous nonconventional methods thus being hope for the future. This had a great impact on emerging battery technology. Lithium-ion batteries are the most magnificent sources available today to store and utilize energy. This is because of their versatility, adaptability, and flexibility. Lithium-ion batteries have been used from microelectronics to automotive and aerospace

application. High energy density, long life, less maintenance compact size are some of their superior characters. With the advent of battery electric vehicles world is witnessing for another automobile revolution. A combination of individual cells to form a battery pack is used to power these electric vehicles. These vehicles use mainly lithium ion 18650 cells. But despite all these merits they still face certain limitations like thermal management and long charging duration. While later need advancement in science and technology former can be solved with the help of smart engineering. An efficiently designed cooling technique with suitable coolant should be able to control the cell temperature. This very important from a performance point of view. Higher temperature can lead to thermal runaway and poor performance thus resulting in poor efficiency. Operating lithium-ion cells at a higher temperature also reduces their overall life with each cycle. Thus temperature control plays an important role and making the need for proper cooling of the cells a quintessential for lithium-ion cells.

APPENDIX I

NOMENCLATURE

T-Temperature; Kelvin –K

$\dot{Q}$-Heat generated per second; WattsW

t-Time; Seconds s

h-Heat transfer coefficient; W/m^2K

α-Thermal Diffusivity; m^2/s

k-Coefficient of Thermal Conductivity; W/mK

r-Radius from symmetry axis; m

β-Coefficient of Thermal Expansion; K^{-1}

g-Acceleration due to gravity; $9.81m/s^2$

D_h-Hydraulic Diameter; m

v-Kinematic Viscosity; m^2/s

μ-Dynamic Viscosity; Pa.s

Re-Reynolds Number

Gr-Grashoff's Number

Pr-Prandtl Number

Nu-Nusselt Number

p-Pressure; Pa

P-Perimeter; m

A-Area; m^2

$\vec{v}$-Velocity; m/s

R-Cell Resistance; Ω

i-Current Density; A/m^3

E-Cell Voltage; V

E_{oc}-Cell open circuit voltage; V

ΔS-Entropy change of cell; J/K

ρ-Density; kg/m^3

c_p-Specific heat capacity; J/kg

τ-Viscous Stress Tensor;N/m^2

S-Strain rate Tensor; $1/s$

$\boldsymbol{u}$-Velocity; m/s

α_p-Thermal Expansion coefficient of Fluid;K^{-1}

SUBSCRIPTS

s-Inner Surface

c-Cross Section

S-Cell surface

f-fluid

REFERENCES

[1] Tao Wang, K.J. Tseng, Jiyun Zhao; Zhongbao Wei.Thermal investigation of lithium-ion battery module with different cell arrangement structures and forced air-cooling strategies. Appl Energy 2014; 134:229e38.

[2] Xun J, Liu R, Jiao K. Numerical and analytical modeling of lithium-ion battery thermal behaviors with different cooling designs. J Power Sources 2013; 233:47e613

[3] Naixing Yang, Xiongwen Zhang, Guojun Li, Dong Hua, Assessment of the forced air-cooling performance for cylindrical lithium-ion battery packs: A comparative analysis between aligned and staggered cell arrangements", Applied Thermal Engineering 80 (2015) 55e65

[4] Ali M Sefidan, Atta Sojoudi, Suvash Saha "Nano fluid-based cooling of cylindrical lithium-ion battery packs employing forced air flow", International Journal of Thermal Sciences 117 (2017) 44e58

[5] Yang Li, Huaqing Xie∗, Wei Yu, and Jing Li,",Liquid cooling of tractive lithium ion batteries pack with nanofluids",Journal of Nanoscience and Nanotechnology Vol. 15, 3206–3211, 2015

[6] Long Cai, Ralph E. White, "Mathematical modeling of a lithium ion battery with thermal effects in COMSOL Inc. Multiphysics (MP) software", Journal of Power Sources 196 (2011) 5985–5989

[7]C.Ziebert, A.Melcher, B.Lei] Methodologies for electrochemical and thermal characterization of Li-ion cells to improve thermal management and prevent thermal runaway"Comsol Conference Munich 2016

[8] Leyuan Yu, Dong Liu, Frank Botz Laminar convective heat transfer of alumina-polyalphaolefin nanofluids containing spherical and non-spherical nanoparticles Experimental Thermal and Fluid Science 37 (2012) 72–83

[9] S. Suresh , K.P. Venkitaraj, P. Selvakumar , M. Chandrasekar ,"Effect of Al2O3–Cu/water hybrid nanofluid in heat transfer", Experimental Thermal and Fluid Science 38 (2012) 54–60

[10]Bittagopal Mondal, Carlos F. Lopez, Partha P. Mukherjee, "Exploring the efficacy of Nano fluids for lithium-ion battery thermal management" International Journal of Heat and Mass Transfer 112 (2017) 779–794

[11]_Adnan M. Hussein , R.A. Bakar , K. Kadirgama, K.V. Sharma _Heat transfer enhancement using nanofluids in an automotive cooling system",_International Communications in Heat and Mass Transfer 53 (2014) 195–202

[12] Hazima Faezaa Ismail ,Siti Fauziah Toha , Nor Aziah Mohd Azubir,NizamHanis Md Ishak,Mohd Khair Hassan ,Babul Salam KSM Ibrahim "Simplified Heat Generation Model for Lithium ion batteryused in Electric Vehicle" Nur IOP Conf. Series: Materials Science and Engineering 53 (2013) 012014

[13] PhD. John Dunning, Prof. Thomas Mackin, Prof. Roland Rozsnyo, Ing. Joel Stoudmann " Heat Generation Modeling of a Lithium Battery: from the Cell, to the Pack on COMSOL Multiphysics" Excerpt from the Proceedings of the 2015 COMSOL Conference in Grenoble

[14] Thanh-Ha Tran , Souad Harmand , Bernard Desmet , Sebastien Filangi "Experimental investigation on the feasibility of heat pipe cooling for HEV/EV lithium-ion battery" Applied Thermal Engineering 63 (2014) 551e558

[15] Guangming Liu • Minggao Ouyang •Languang Lu • Jianqiu Li • Xuebing Han J "Analysis of the heat generation of lithium-ion battery during charging and discharging considering different influencing factors" Therm Anal Calorim DOI 10.1007/s10973-2013-3599-90

[16] Rajib Mahamud, Chanwoo Park "Reciprocating air flow for Li-ion battery thermal management to improve temperature uniformity" Journal of Power Sources 196 (2011) 5685–5696

[17] R. Kizilel , A. Lateef , R. Sabbah , M.M. Farid , J.R. Selman , S. Al-Hallaj "Passive control of temperature excursion and uniformity in high-energy Li-ion battery packs at high current and ambient temperature"; Journal of Power Sources 183 (2008) 370–375

[18] Liwu Fan , J.M. Khodadadi , A.A. Pesaran "A parametric study on thermal management of an air-cooled lithium-ion battery module for plug-in hybrid electric vehicles"Journal of Power Sources 238 (2013) 301e312

[19] Kothandaraman, C.P., and S. Subramanyan Heat and Mass Transfer Databook, ISBN 9789386649300, 9386649306 Edition:9th, 2018.

[20]SimScaleDocspage,"https://www.simscale.com/docs/content/simulation/analysis_types/OF_conjugateHeatTransfer.html"